Meteoritics & Planetary Science 38, Nr 9, 1399–1418 (2003)
Abstract available online at http://meteoritics.org

Microdistribution of primordial Ne and Ar in fine-grained rims, matrices, and dark inclusions of unequilibrated chondrites—Clues on nebular processes

Nadia VOGEL,[1†*] Rainer WIELER,[1] Addi BISCHOFF,[2] and Heinrich BAUR[1]

[1]Institute for Isotope Geology and Mineral Resources, Sonnegstrasse 5, NO C61, ETH Zürich, 8092 Zürich, Switzerland
[2]Institute of Planetology, Wilhelm-Klemm-Str. 10, University of Münster, 48149 Münster, Germany
[†]Present address: Berkeley Geochronology Center, 2455 Ridge Road, Berkeley, California 94709, USA
[*]Corresponding author. E-mail: nvogel@bgc.org

(Received 27 June 2002; revision accepted 22 May 2003)

Abstract–The low temperature fine-grained material in unequilibrated chondrites, which occurs as matrix, rims, and dark inclusions, carries information about the solar nebula and the earliest stages of planetesimal accretion. The microdistribution of primordial noble gases among these components helps to reveal their accretionary and alteration histories. We measured the Ne and Ar isotopic ratios and concentrations of small samples of matrix, rims, and dark inclusions from the unequilibrated carbonaceous chondrites Allende (CV3), Leoville (CV3), and Renazzo (CR2) and from the ordinary chondrites Semarkona (LL3.0), Bishunpur (LL3.1), and Krymka (LL3.1) to decipher their genetic relationships. The primordial noble gas concentrations of Semarkona, and—with certain restrictions—also of Leoville, Bishunpur, and Allende decrease from rims to matrices. This indicates a progressive accretion of nebular dust from regions with decreasing noble gas contents and cannot be explained by a formation of the rims on parent bodies. The decrease is probably due to dilution of the noble-gas-carrying phases with noble-gas-poor material in the nebula. Krymka and Renazzo both show an increase of primordial noble gas concentrations from rims to matrices. In the case of Krymka, this indicates the admixture of noble gas-rich dust to the nebular region from which first rims and then matrix accreted. This also explains the increase of the primordial elemental ratio $^{36}Ar/^{20}Ne$ from rims to matrix. Larger clasts of the noble-gas-rich dust form macroscopic dark inclusions in this meteorite, which seem to represent unusually pristine material. The interpretation of the Renazzo data is ambiguous. Rims could have formed by aqueous alteration of matrix or—as in the case of Krymka—by progressive admixture of noble gas-rich dust to the reservoir from which the Renazzo constituents accreted.

The Leoville and Krymka dark inclusions, as well as one dark inclusion of Allende, show noble gas signatures different from those of the respective host meteorites. The Allende dark inclusion probably accreted from the same region as Allende rims and matrix but suffered a higher degree of alteration. The Leoville and Krymka dark inclusions must have accreted from regions different from those of their respective rims and matrices and were later incorporated into their host meteorites. The noble gas data imply a heterogeneous reservoir with respect to its primordial noble gas content in the accretion region of the studied meteorites. Further studies will have to decide whether these differences are primary or evolved from an originally uniform reservoir.

INTRODUCTION

Carbonaceous and ordinary chondrites (CCs, OCs) contain variable proportions of fine-grained opaque material that is interstitial to larger entities such as chondrules or inclusions. This "matrix-like" material is mainly composed of solar nebula condensates and reprocessed matter such as chondrule debris (Alexander 1989; Brearley 1996; Brenker et al. 2000; Buseck and Hua 1993; Huss et al. 1981; Scott et al. 1988). Additionally, it contains presolar grains (Anders and Zinner 1993; Huss and Lewis 1995). The matrix-like material eventually suffered alteration both in the solar nebula and later on parent bodies (Bischoff 1998; Brearley and Jones 1998; Buseck and Hua 1993). In type 2 and 3 chondrites however, this material escaped major thermal parent body alteration. Therefore, the matrix in these meteorites still

carries information about the solar nebula and the earliest stages of planetesimal accretion (e.g., Buseck and Hua 1993).

The matrix-like material is the host for most primordial noble gases in unequilibrated chondrites (Huss et al. 1996; Smith et al. 1977). These reside in two main carrier phases: presolar diamonds containing the so called HL component (Huss and Lewis 1994) and the enigmatic carbonaceous "phase Q" (Busemann et al. 2000; Ott 2002; Ott et al. 1981), which is the carrier of the "normal" primordial noble gas component (Lewis et al. 1975; Ott 2002). While presolar diamonds carry the bulk of the primordial He and Ne (Huss and Lewis 1994), the major part of the primordial heavier noble gases Ar, Kr, and Xe reside in phase Q (Lewis et al. 1975). The Ne and Ar isotopic and elemental noble gas compositions for Q and HL gases, as well as for other reservoirs relevant here, are given in Table 1. Based on textural criteria, matrix-like material can be further subdivided (e.g., Brearley and Jones 1998; Metzler et al. 1992; Scott et al. 1988; Semenenko et al. 2001; Weisberg and Prinz 1998). Aside from its most common occurrence as an opaque groundmass (termed "matrix" in the following), fine-grained concentric rims ("rims") around larger objects such as chondrules and inclusions are common (e.g., MacPherson et al. 1985; Metzler and Bischoff 1989; Metzler et al. 1992). In CM chondrites, the highest concentrations of primordial noble gases are found in this rim component (Nakamura et al. 1999b). The third occurrence of matrix-like material is as macroscopically distinct dark lumps and clasts (Brearley and Jones 1998; Endress et al. 1994; Scott et al. 1984) collectively termed "dark inclusions" (DIs). The genetic relationships between matrices, rims, and DIs are not yet well-understood.

Here, we report the results of Ne and Ar analyses of matrix, rims, and several DIs from Allende (CV3), Leoville (CV3), Renazzo (CR2), Semarkona (LL3.0), Bishunpur (LL3.1), and Krymka (LL3.1). Apart from these "gas-rich" components, we also analyzed high temperature objects like chondrules and refractory inclusions (CAIs) containing much lower concentrations of primordial noble gases. These data, so far, have been published in abstracts (Vogel et al. 2000, 2001a, 2001b, 2002) and a Ph.D. thesis (Vogel 2003) and will be comprehensively discussed in future papers.

The primordial noble gas concentrations and isotopic and elemental abundances of matrices, rims, and DIs provide information about conditions and processes during the accretion of the meteorite parent bodies, such as mixing and alteration both in the solar nebula and on larger bodies. Furthermore, the primordial noble gas signatures hint on the genetic relationships between the above components.

SAMPLES AND EXPERIMENTAL PROCEDURE

Samples

The samples had to meet the following requirements: 1) to ensure a small degree of alteration, only type 2 and 3 chondrites were selected; 2) the different components had to be large enough to enable a proper separation without cross-contamination with adjacent material, which precluded CM chondrites; 3) the samples should not contain solar wind (SW) noble gases acquired in a regolith, since these would obscure the primordial gas components; 4) the exposure ages of the samples should be short to minimize the contribution of cosmogenic noble gases. Krymka, with an exposure age of ~26 Ma, does not fulfil the latter requirement. Nevertheless, Krymka was included, since it is among the least altered chondrites and the thick section investigated contains a DI with extraordinarily primitive textures (Semenenko et al. 2001). During the study, we found that the DI contained extremely high primordial noble gas concentrations, which were not affected significantly by the cosmogenic contributions. However, a large part of the noble gases in the

Table 1. Ne and Ar isotopic and elemental compositions of phase Q, presolar diamonds (HL), and other reservoirs relevant here.[a]

	$^{20}Ne/^{22}Ne$	$^{21}Ne/^{22}Ne$	$^{36}Ar/^{38}Ar$	$^{20}Ne/^{36}Ar$	References
Q	10.05(5)–10.7(2)	0.0291(16)–0.0294(10)	5.34(2)	14–84	Busemann et al. 2000
HL	8.50(6)	0.036(1)	4.41(6)	0.103(42)	Huss and Lewis 1994
SW	13.8(1)	0.0328(5)	5.58(3)	~0.04	Benkert et al. 1993
Air	9.80(8)	0.0290(3)	5.32(1)	1.9	a) Eberhardt et al. 1965; b) Nier
	a)	a)	b)	c)	1950; c) Ozima and Podosek 2002
GCR (typical range)	0.70–0.93	0.80–0.95	0.65(3)		Wieler 2002
$^{1}Allende_{cos}$	0.83(2)	0.93(5)			Vogel 2003
$^{1}Leoville_{cos}$	0.835(8)	0.93(2)			Vogel 2003
$^{1}Renazzo_{cos}$	0.81(2)	0.87 (6)			Vogel 2003
$^{1}Semarkona_{cos}$	0.81(1)	0.87(4)			Vogel 2003
$^{1}Bishunpur_{cos}$	0.824(8)	0.90(2)			Vogel 2003
$^{1}Krymka_{cos}$	0.831(4)	0.92(1)			Vogel 2003

[a]The numbers in parentheses represent uncertainties in units of the least significant digit.

[l]The cosmogenic $^{20}Ne/^{22}Ne$ and $^{21}Ne/^{22}Ne$ for each meteorite are average values determined in this work from chondrules of the respective meteorites. The uncertainties represent the standard deviations of the values.

Krymka matrix and rims, which were measured for comparison, were indeed of cosmogenic origin.

Before sampling, most of the cut and polished meteorite chips were mapped by SEM (CamScan CS44LB with a four-quadrant BSE detector). To avoid contamination of the samples with carbon, the chips were not coated. Examples of the images with selected sample locations are given in Figs. 1–4.

From the chips, small samples (~20 to ~600 μg) of matrix, rims, and DIs were carefully hand-separated under a binocular microscope. The OCs generally contain much less fine-grained material (up to 15 vol%; Brearley 1996) than the

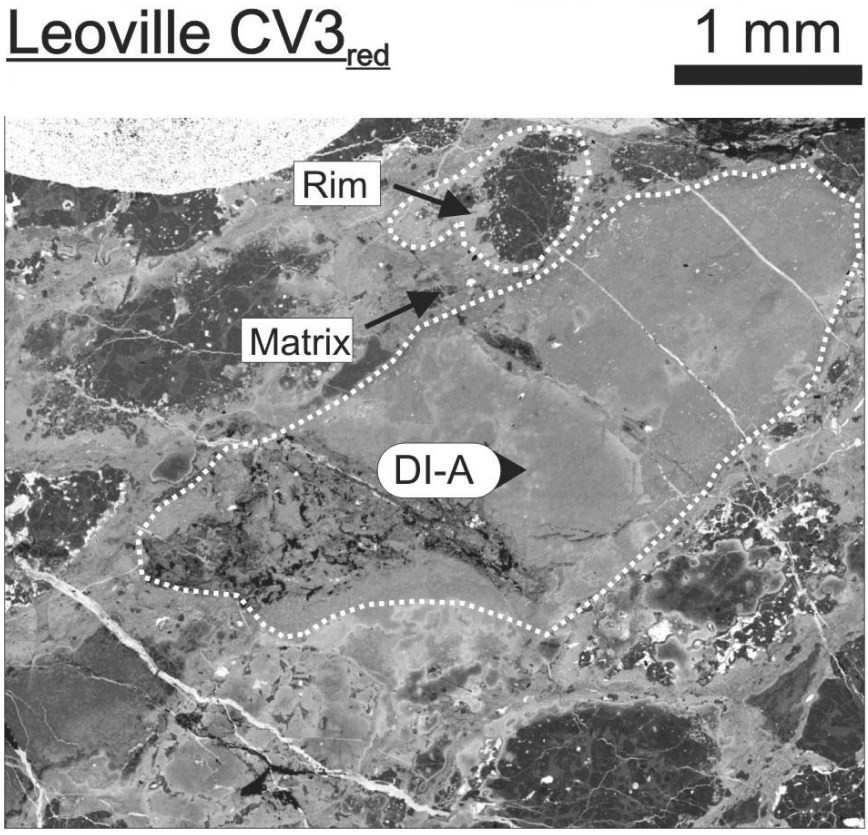

Fig. 1. Composite BSE image of Leoville showing the fine-grained dark inclusion L-DI-A. Typical fine-grained rims around chondrules and slightly darker interstitial matrix (not separated at this location) are also visible.

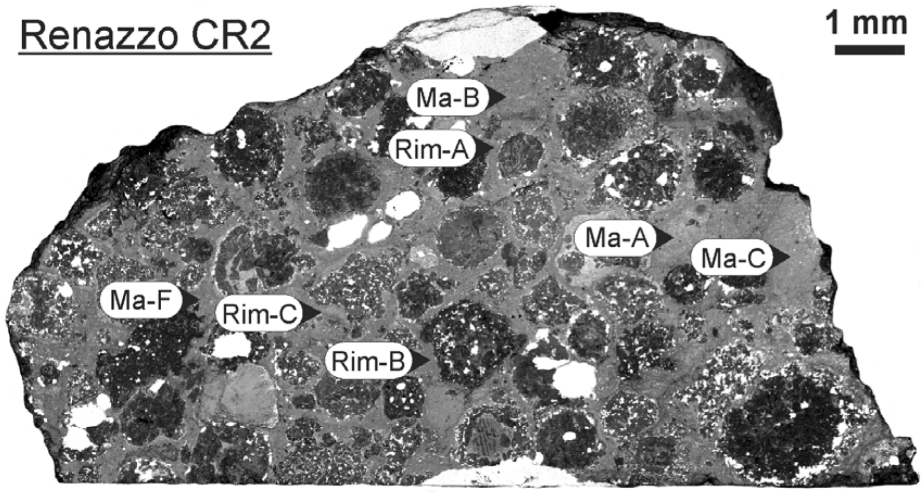

Fig. 2. Composite BSE image of the studied chip of Renazzo with all sample locations. Rims and matrix were generally easy to separate.

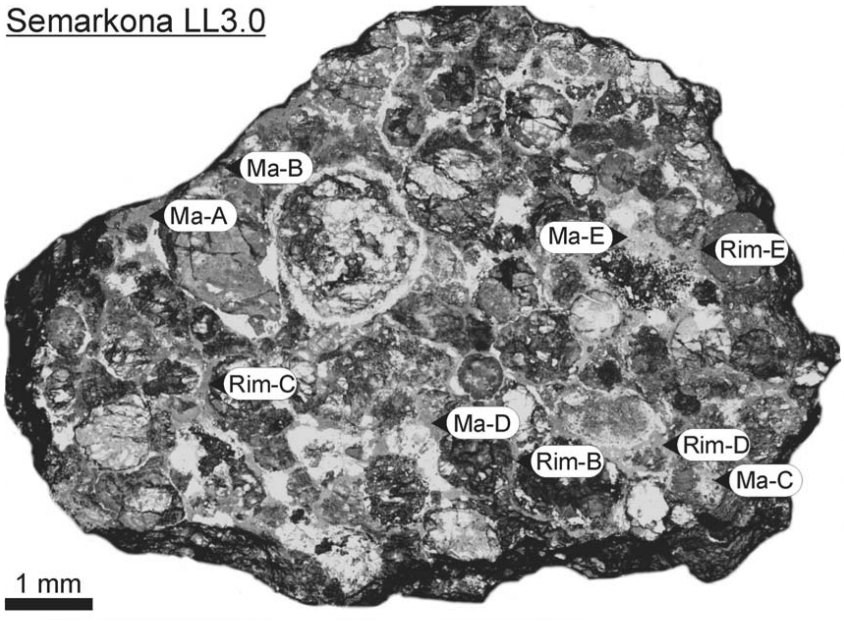

Fig. 3. Composite BSE image of the studied chip of Semarkona with all sample locations. Note the small amount of fine-grained rim and interstitial matrix material and the overall abundance of light-colored, metal-sulphide-rich rims and blebs.

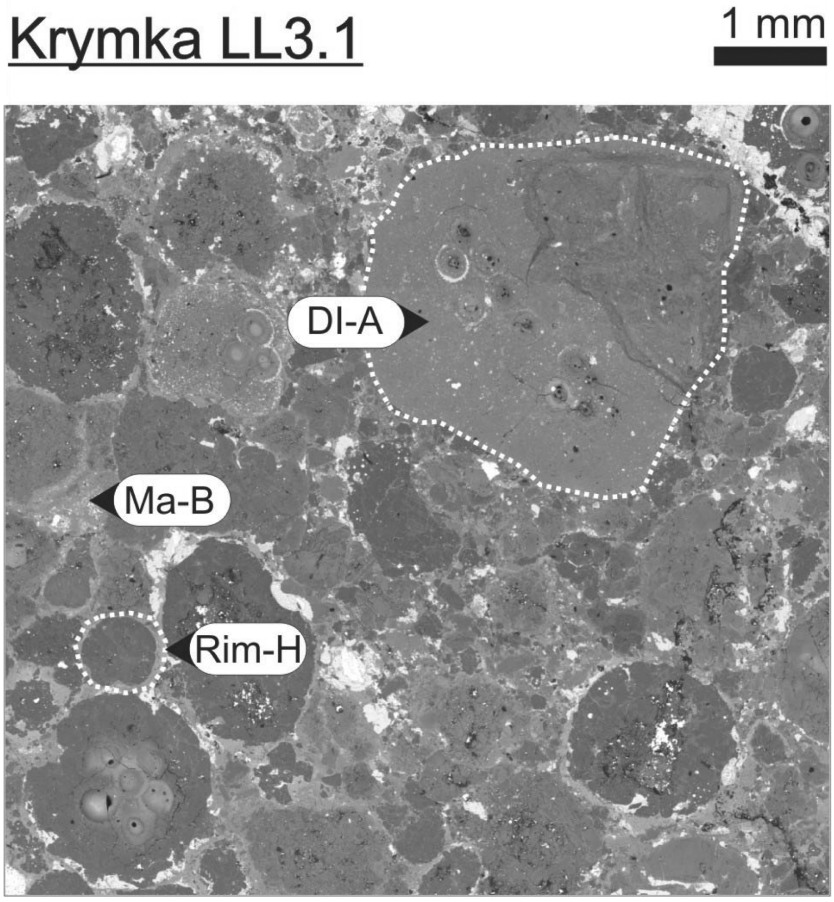

Fig. 4. Composite BSE image of Krymka showing the fine-grained dark inclusion K-DI-A and the sample locations for one matrix and one rim sample. Small round holes within the dark inclusion and some chondrules are from in situ laser analyses (not reported here).

CV chondrites (~40 vol%; Scott et al. 1996), Therefore, for some OCs, only few samples of rims and matrix could be obtained. Matrix and rim material were not always easy to separate from each other, since the transition between the two components is often blurred. Therefore, the samples may not always represent the pure component but can be cross-contaminated to some degree. Furthermore, the third dimension could not be controlled, which in a few cases may have led to a substantial contamination of a sample. All samples were weighed and put into the storage holes of aluminium sample holders, each with the capacity to carry 9 samples.

The nomenclature of the samples is as follows: the first letter indicates the meteorite (A = Allende, L = Leoville, R = Renazzo, S = Semarkona, B = Bishunpur, K = Krymka). The specification of the component follows (Ma = fine-grained opaque matrix, Rim = fine-grained rim material, DI = dark inclusion). The next letter (a–h) distinguishes the different samples of one component in the respective meteorite; the numbers (1–9) attached to these letters indicate different analyses of the same object.

Gas Extraction and Measurements

After a bake out in vacuum (~24 hr at 100°C) to remove atmospheric gases, the noble gases were extracted by melting the samples with a Nd-YAG-laser in CW-mode (λ = 1064 nm). During the melting, the output power of the laser was individually adjusted (20–30 W). The melting was observed on a video-monitor and generally took 60–300 sec depending on the size of the sample and its volatile content. To avoid the heating of adjacent samples, the sample holder was water-cooled. Shots on already degassed samples or on empty holes proved that no measurable amounts of noble gases from neighboring samples were extracted.

The gas was purified with the help of a cold trap at liquid N_2 temperature (–196°C) and two Ti/Zr getters. An activated charcoal trap cooled with liquid N_2 was used to separate the He-Ne- from the Ar-fraction. Noble gases were measured on a non-commercial mass spec-trometer (90°, 21 cm radius) equipped with an ion counting electron multiplier and a Faraday cup.

The gas was ionized by electrons with the energy of only 45 eV to reduce the double ionization of ^{40}Ar and $^{12}C^{16}O_2$. Thus, only ~0.1% of the measured ^{40}Ar (Busemann 1998) and ~0.05% of the measured $^{44}CO_2$ are doubly ionized and interfere with ^{20}Ne and ^{22}Ne, respectively. The interference correction generally accounts for less than 1% of the measured ^{20}Ne and ^{22}Ne in the samples. The mass resolution of the spectrometer is sufficient to resolve ^3He and HD as well as ^{20}Ne and $^1H_2{}^{18}O$. Therefore, no interference corrections for these background species are necessary. $^{35, 37}Cl$ signals were constantly low during the Ar analyses of samples and blanks. Therefore, possible small interferences of $^{35}Cl^1H$ with ^{36}Ar and $^{37}Cl^1H$ with ^{38}Ar would have been corrected via the blank subtraction.

A more detailed description of the noble gas extraction line and the mass spectrometer can be found in Vogel (2003).

Blanks and Corrections for Cosmogenic Noble Ggases

"Cold blanks" were determined by simulating a sample extraction procedure without a laser beam. Average ^{20}Ne and ^{36}Ar cold blanks over 2 years were $(1.1 \pm 0.6) \times 10^{-13}$ and $(1.4 \pm 0.7) \times 10^{-13}$ cm^3 STP, respectively. "S-blanks" were also measured by reheating an already extracted sample. Thereby, extraction time and laser energy were identical to the respective values in adjacent sample runs, as blank signals significantly depend on these parameters. S-blanks served to verify the completeness of the noble gas extraction. Additional "a-blanks," where the laser was applied on empty holes of the aluminium sample holder, yielded reliable blank signals, since it was not always clear whether the increase of an s-blank was due to small amounts of residual sample gas or simply to the use of the laser. Typical ^{20}Ne and ^{36}Ar amounts of sample gas-free s-blanks were only slightly higher than the cold blanks, $(1.2 \pm 0.6) \times 10^{-13}$ and $(1.8 \pm 0.7) \times 10^{-13}$ cm^3 STP, respectively. Generally, an "s-blank" was performed for every sample and was used for the blank-correction, except in the cases where it still released discernible amounts of sample gas. These were added to the noble gas amounts of the nominal sample extraction steps after both had been corrected with a cold- or an a-blank. Despite the small sample amounts, the ^{20}Ne blanks contributed only 2% on average to the measured amounts of ^{20}Ne and never exceeded 17%. The ^{36}Ar blanks contributed 0.6% on average to the measured ^{36}Ar gas amounts, and the maximum contribution was 8%.

The extracted gases represent mixtures of primordial and cosmogenic noble gases. To obtain the primordial ^{20}Ne and ^{36}Ar portions ($^{20}Ne_{prim}$, $^{36}Ar_{prim}$), the measured gas amounts were corrected for cosmogenic contributions by two-component deconvolution. To calculate the $^{20}Ne_{prim}$, a primordial $^{21}Ne/^{22}Ne$ of 0.03 and individual primordial $^{20}Ne/^{22}Ne$ ratios for every meteorite adopted from regressions in Ne-3-isotope-plots were used (numbers in boxes in Fig. 5). The cosmogenic Ne isotopic composition varies significantly with the exposure depth of a given sample (Wieler 2002). Therefore, we individually corrected the samples of each meteorite with average cosmogenic Ne isotopic ratios from chondrules of the same specimens, which did not contain significant amounts of $^{20}Ne_{prim}$ (Table 1). The average cosmogenic contribution to the measured ^{20}Ne was 19% and increased up to 65% for some very gas-poor Bishunpur and Krymka samples, resulting in larger uncertainties of the $^{20}Ne_{prim}$ concentrations of these samples (Tables 2–7).

To calculate the $^{36}Ar_{prim}$ we used the $^{36}Ar/^{38}Ar$ ratio of phase Q: 5.34 (Table 1). All samples show measured $^{36}Ar/^{38}Ar$ ratios close to this value, indicating only a minor

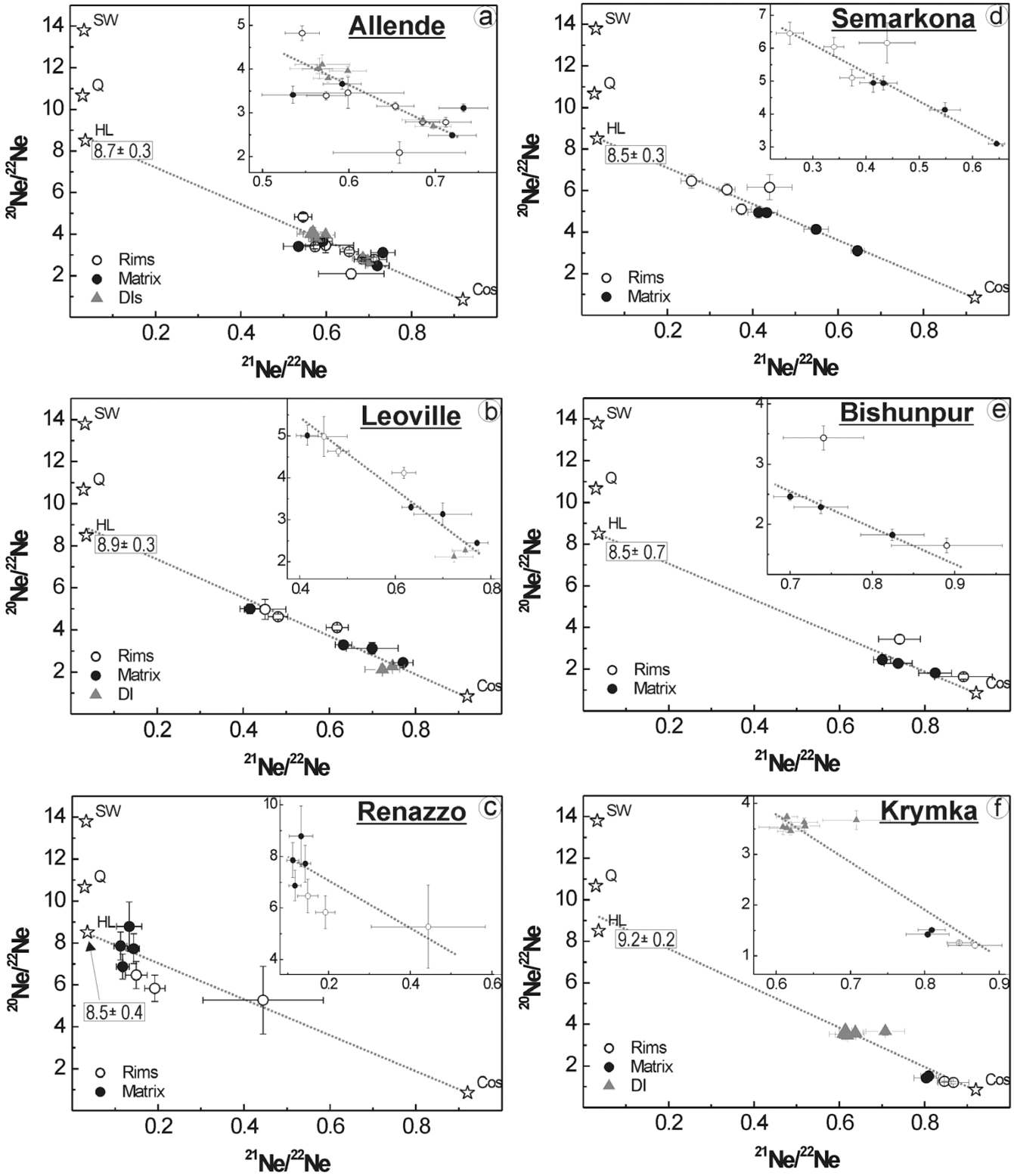

Fig. 5. Ne isotopic composition of rims, matrix, and dark inclusions of Allende, Leoville, Renazzo, Semarkona, Bishunpur, and Krymka. The Ne composition of solar wind (SW), phase Q (Q), presolar diamonds (HL), and typical cosmogenic ratios are listed in Table 1. The numbers in the boxes are the primordial $^{20}Ne/^{22}Ne$ composition (adopted $^{21}Ne/^{22}Ne$ ratio: 0.03) from the calculated mixing lines of all data points of each meteorite, respectively. The inserts are close-ups of the locations of the data points. See the text for further explanations.

Table 2. Ne and Ar isotopic, elemental, and primordial composition of Allende rims, matrix, and dark inclusions. The contributions of blanks to $^{20}Ne_{prim}$ and $^{36}Ar_{prim}$ and the portion of cosmogenic gases at the measured ^{20}Ne ($^{20}Ne_{meas}$) are also given in %.[a]

Name	Weight (g) $\times 10^{-4}$	$^{20}Ne_{meas}$	$^{36}Ar_{meas}$	$^{20}Ne/^{22}Ne$	$^{21}Ne/^{22}Ne$	$^{36}Ar/^{38}Ar$	$^{20}Ne_{prim}$	Blank contr. to $^{20}Ne_{prim}$	Cosmogenic contr. to $^{20}Ne_{meas}$	$^{36}Ar_{prim}$	Blank contr. to $^{36}Ar_{prim}$	$(^{36}Ar/^{20}Ne)_{prim}$
A-DI-A1	5.8(3)	6.1(3)	24(1)	2.70(6)	0.70(2)	5.05(5)	4.6(4)	0.5	23	24(1)	0.2	5.1(3)
A-DI-A2	1.53(8)	6.2(3)	24(1)	2.84(9)	0.69(2)	5.07(5)	4.9(5)	20.8	21	24(1)	1.0	4.9(4)
A-DI-B1	1.202(5)	10.6(2)	35.4(2)	4.1(2)	0.57(3)	5.09(6)	9.3(5)	0.8	12	35.1(3)	0.3	3.8(2)
A-DI-B2	3.156(5)	10.1(1)	32.3(2)	4.0(1)	0.60(2)	5.10(6)	8.8(5)	0.4	13	32.0(3)	0.3	3.6(2)
A-DI-B3	3.176(5)	10.7(2)	31.4(2)	3.79(8)	0.58(2)	5.17(3)	9.3(5)	0.2	14	31.3(3)	0.1	3.4(2)
A-DI-C1	3.708(5)	11.1(1)	33.8(2)	4.0(1)	0.56(2)	5.11(7)	9.8(5)	0.6	12	33.5(3)	0.3	3.4(2)
A-DI-C2	1.367(5)	11.0(2)	34.8(2)	4.0(2)	0.57(3)	5.20(5)	9.7(5)	0.8	12	34.6(2)	0.3	3.6(2)
A-Ma-A1	0.99(5)	9.7(5)	26(1)	3.7(1)	0.59(2)	5.25(7)	8.3(7)	1.7	14	26(1)	1.0	3.1(2)
A-Ma-A2	0.58(3)	9.5(5)	27(1)	3.4(2)	0.54(4)	5.16(7)	8.2(7)	2.9	14	27(1)	1.6	3.3(2)
A-Ma-B	1.27(1)	7.6(2)	24.3(3)	3.11(9)	0.73(3)	5.14(4)	6.1(5)	1.6	20	24.1(3)	0.4	4.0(3)
A-Ma-C	2.23(2)	6.8(1)	18.8(2)	2.49(6)	0.72(3)	5.06(4)	5.0(4)	1.2	27	18.6(2)	0.4	3.7(3)
A-Rim-A1	*0.24(1)*	*5.3(4)*	*11.6(6)*	*2.1(2)*	*0.66(8)*	*5.0(2)*	*3.8(6)*	*13.2*	*28*	*11.5(7)*	*7.6*	*3.0(5)*
A-Rim-A2	0.35(2)	9.8(5)	28(1)	3.5(4)	0.60(7)	5.3(1)	8.3(7)	7.5	15	27(1)	2.6	3.3(2)
A-Rim-B1	2.5(1)	7.7(4)	24(1)	3.16(9)	0.65(2)	5.14(5)	6.3(5)	1.0	19	23(1)	0.5	3.7(2)
A-Rim-B2	2.3(1)	9.3(5)	28(1)	3.39(9)	0.57(2)	5.18(6)	7.9(6)	0.7	15	28(1)	0.4	3.5(2)
A-Rim-C1	1.03(1)	6.6(2)	19.1(2)	2.8(1)	0.71(3)	5.04(6)	5.2(4)	2.3	22	18.9(3)	0.5	3.7(3)
A-Rim-C2	0.821(8)	7.0(2)	22.2(3)	2.79(8)	0.69(2)	5.05(5)	5.5(4)	2.6	21	22.0(3)	0.6	4.0(3)
A-Rim-D	1.23(2)	14.0(3)	41.0(6)	4.8(2)	0.55(2)	5.10(4)	12.6(7)	0.7	10	40.7(7)	0.2	3.2(2)

[a]Gas concentrations are given in units of (10^{-8} cm^3 STP/g). The correction of the measured ^{20}Ne and ^{36}Ar concentrations for cosmogenic contributions is explained in the text. Italics indicate samples that are discarded from the discussion of primordial noble gas systematics. See the text for further explanation.

Table 3. Ne and Ar isotopic, elemental, and primordial composition of Leoville rims, matrix, and a dark inclusion. The contributions of blanks to $^{20}Ne_{prim}$ and $^{36}Ar_{prim}$ and the portion of cosmogenic gases at the measured ^{20}Ne ($^{20}Ne_{meas}$) are also given in %.[a]

Name	Weight (g) $\times 10^{-4}$	$^{20}Ne_{meas}$	$^{36}Ar_{meas}$	$^{20}Ne/^{22}Ne$	$^{21}Ne/^{22}Ne$	$^{36}Ar/^{38}Ar$	$^{20}Ne_{prim}$	Blank contr. to $^{20}Ne_{prim}$	Cosmogenic contr. to $^{20}Ne_{meas}$	$^{36}Ar_{prim}$	Blank contr. to $^{36}Ar_{prim}$	$(^{36}Ar/^{20}Ne)_{prim}$
L-DI-A3	0.625(7)	11.0(2)	17.9(2)	2.27(4)	0.75(3)	4.70(5)	7.7(6)	1.4	30	17.5(5)	1.1	2.3(2)
L-DI-A4	0.257(6)	10.8(6)	21.2(5)	2.1(1)	0.72(4)	4.87(7)	7.5(9)	3.6	31	21(1)	3.4	2.8(4)
L-Ma-B	0.184(9)	25(2)	497(25)	3.1(3)	0.70(6)	5.28(5)	20(3)	5.5	18	495(51)	0.3	24(4)
L-Ma-C1	*0.11(1)*	*42(5)*	*1037(127)*	*5.0(2)*	*0.42(2)*	*5.38(4)*	*39(5)*	*1.0*	*7*	*1036(262)*	*0.1*	*27(6)*
L-Ma-C2	1.034(5)	16.1(3)	310(2)	2.45(6)	0.77(2)	5.32(4)	11.6(8)	0.6	28	311(4)	0.1	27(2)
L-Ma-C3	1.239(7)	25.4(3)	581(5)	3.30(8)	0.63(2)	5.33(4)	21(1)	0.3	18	580(9)	0.0	28(2)
L-Rim-B	0.153(8)	37(4)	814(41)	5.0(5)	0.45(5)	5.35(5)	34(5)	4.0	7	813(84)	0.2	24(4)
L-Rim-C1	*1.071(5)*	*16.8(2)*	*331(3)*	*4.1(1)*	*0.62(3)*	*5.35(3)*	*14.6(8)*	*0.6*	*13*	*331(5)*	*0.0*	*23(1)*
L-Rim-C2	0.450(5)	32.2(6)	652(8)	4.6(1)	0.48(2)	5.32(3)	29(2)	0.7	9	652(16)	0.0	22(1)

[a]Gas concentrations are given in units of (10^{-8} cm^3 STP/g). The correction of the measured ^{20}Ne and ^{36}Ar concentrations for cosmogenic contributions is explained in the text. Italics indicate samples that are discarded from the discussion of primordial noble gas systematics. See the text for further explanation.

Table 4. Ne and Ar isotopic, elemental, and primordial composition of Renazzo rims and matrix. The contributions of blanks to $^{20}Ne_{prim}$ and $^{36}Ar_{prim}$ and the portion of cosmogenic gases at the measured ^{20}Ne ($^{20}Ne_{meas}$) are also given in %.[a]

Name	Weight (g) ×10^{-4}	$^{20}Ne_{meas}$	$^{36}Ar_{meas}$	$^{20}Ne/^{22}Ne$	$^{21}Ne/^{22}Ne$	$^{36}Ar/^{38}Ar$	$^{20}Ne_{prim}$	Blank contr. to $^{20}Ne_{prim}$	Cosmogenic contr. to $^{20}Ne_{meas}$	$^{36}Ar_{prim}$	Blank contr. to $^{36}Ar_{prim}$	$(^{36}Ar/^{20}Ne)_{prim}$
R-Ma35-A	0.485(1)	20.9(7)	90.9(5)	6.9(6)	0.12(1)	5.29(3)	21(2)	0.6	1	90.7(7)	0.3	4.4(3)
R-Ma35-B	0.43(3)	23(1)	80(5)	7.9(7)	0.11(2)	5.27(3)	23(2)	0.9	1	80(5)	0.2	3.5(2)
R-Ma36-C2	0.809(8)	16.3(5)	72.4(7)	7.7(7)	0.14(1)	5.27(5)	16(1)	0.6	1	72.3(8)	0.2	4.5(3)
R-Ma37-F	0.21(2)	22(2)	82(8)	9(1)	0.13(3)	5.31(6)	22(3)	1.2	1	82(8)	0.9	3.8(2)
R-Rim35-A	0.27(1)	14.7(7)	53(2)	6.5(6)	0.15(3)	5.30(6)	14(1)	2.8	2	53(2)	1.4	3.7(3)
R-Rim35-B	0.344(8)	16.1(5)	64(2)	5.8(6)	0.19(2)	5.29(3)	16(1)	0.7	3	64(2)	0.4	4.1(2)
R-Rim36-C	0.135(1)	13.7(4)	50.3(5)	5(2)	0.4(1)	5.21(7)	13(1)	3.5	8	50.0(6)	1.3	3.9(3)

[a]Gas concentrations are given in units of (10^{-8} cm^3 STP/g). The correction of the measured ^{20}Ne and ^{36}Ar concentrations of cosmogenic contributions is explained in the text.

Table 5. Ne and Ar isotopic, elemental, and primordial composition of Semarkona rims and matrix. The contributions of blanks to $^{20}Ne_{prim}$ and $^{36}Ar_{prim}$ and the portion of cosmogenic gases at the measured ^{20}Ne ($^{20}Ne_{meas}$) are also given in %.[a]

Name	Weight (g) ×10^{-4}	$^{20}Ne_{meas}$	$^{36}Ar_{meas}$	$^{20}Ne/^{22}Ne$	$^{21}Ne/^{22}Ne$	$^{36}Ar/^{38}Ar$	$^{20}Ne_{prim}$	Blank contr. to $^{20}Ne_{prim}$	Cosmogenic contr. to $^{20}Ne_{meas}$	$^{36}Ar_{prim}$	Blank contr. to $^{36}Ar_{prim}$	$(^{36}Ar/^{20}Ne)_{prim}$
S-Ma-A	2.93(2)	12.3(2)	131(1)	3.10(7)	0.65(2)	5.30(4)	9.9(6)	0.3	19	131(1)	0.1	13.2(3)
[1]"S-Ma-B"	1.56(2)	25.5(4)		5.7(2)	0.39(1)		24(2)	0.4	6			
S-Ma-C	0.711(4)	16.5(4)	201(1)	4.1(2)	0.55(3)	5.34(4)	15(1)	1.8	12	201(2)	0.2	13.9(4)
S-Ma-D	0.383(2)	12.0(2)	171(2)	4.9(2)	0.43(3)	5.30(6)	11.1(7)	0.5	8	170(2)	0.2	15.3(3)
S-Ma-E	0.925(1)	15.4(3)	222(2)	4.9(3)	0.41(3)	5.33(6)	14(1)	0.9	8	221(2)	0.1	15.5(4)
S-Rim-B	0.38(2)	21(1)	273(14)	6.5(3)	0.26(3)	5.34(4)	20(2)	1.8	3	273(14)	0.3	13.7(3)
S-Rim-C	0.58(3)	22(1)	266(12)	5.1(3)	0.37(2)	5.36(4)	20(2)	1.2	6	266(12)	0.1	13.2(3)
S-Rim-D	0.495(4)	24.6(7)	338(4)	6.0(3)	0.34(2)	5.36(6)	23(2)	1.1	5	337(4)	0.1	14.4(5)
S-Rim-E	0.176(7)	26(1)	362(15)	6.2(6)	0.44(5)	5.34(5)	24(2)	1.5	6	361(15)	0.2	15.0(5)

[a]Gas concentrations are given in units of (10^{-8} cm^3 STP/g). The correction of the measured ^{20}Ne and ^{36}Ar concentrations of cosmogenic contributions is explained in the text. [1]"S-Ma-B" is very probably a mislabeled rim sample, characterized by high $^{20}Ne_{prim}$ concentrations in the range of rim data and also rim-like He (not shown) and Ne isotopic ratios. It was originally separated as "material surrounding a chondrule." No Ar data exists for this sample due to technical problems during the noble gas analysis.

Table 6. Ne and Ar isotopic, elemental, and primordial composition of Bishunpur rims and matrix. The contributions of blanks to $^{20}Ne_{prim}$ and $^{36}Ar_{prim}$ and the portion of cosmogenic gases at the measured ^{20}Ne ($^{20}Ne_{meas}$) are also given in %.[a]

Name	Weight (g) ×10^{-4}	$^{20}Ne_{meas}$	$^{36}Ar_{meas}$	$^{20}Ne/^{22}Ne$	$^{21}Ne/^{22}Ne$	$^{36}Ar/^{38}Ar$	$^{20}Ne_{prim}$	Blank contr. to $^{20}Ne_{prim}$	Cosmogenic contr. to $^{20}Ne_{meas}$	$^{36}Ar_{prim}$	Blank contr. to $^{36}Ar_{prim}$	$(^{36}Ar/^{20}Ne)_{prim}$
B-Ma-A	4.88(1)	7.9(1)	110.9(6)	2.46(6)	0.70(2)	5.29(3)	5.9(6)	0.8	25	110.9(8)	0.0	19(2)
B-Ma-B	1.44(1)	9.1(2)	143(1)	2.3(1)	0.74(3)	5.29(4)	6.5(9)	2.6	29	143(1)	0.0	22(3)
B-Ma-E	0.710(7)	6.2(2)	85(1)	1.8(1)	0.82(4)	5.35(4)	3.6(6)	3.2	42	85(1)	0.3	23(4)
B-Rim-D	*0.47(2)*	*4.4(3)*	*39(2)*	*1.6(1)*	*0.89(7)*	*5.23(6)*	*2.2(4)*	*8.9*	*51*	*39(2)*	*1.2*	*18(3)*
B-Rim-G	0.602(6)	10.4(3)	184(2)	3.4(2)	0.74(5)	5.30(4)	8(1)	2.0	20	183(2)	0.2	22(3)

[a]Gas concentrations are given in units of (10^{-8} cm^3 STP/g). The correction of the measured ^{20}Ne and ^{36}Ar concentrations of cosmogenic contributions is explained in the text. Italics indicate samples that are discarded from the discussion of primordial noble gas systematics. See the text for further explanation.

Table 7. Ne and Ar isotopic, elemental, and primordial composition of Krymka rims and matrix. The contributions of blanks to $^{20}Ne_{prim}$ and $^{36}Ar_{prim}$ and the portion of cosmogenic gases at the measured ^{20}Ne ($^{20}Ne_{meas}$) are also given in %.[a]

Name	Weight (g) $\times 10^{-4}$	$^{20}Ne_{meas}$	$^{36}Ar_{meas}$	$^{20}Ne/^{22}Ne$	$^{21}Ne/^{22}Ne$	$^{36}Ar/^{38}Ar$	$^{20}Ne_{prim}$	Blank contr. to $^{20}Ne_{prim}$	Cosmogenic contr. to $^{20}Ne_{meas}$	$^{36}Ar_{prim}$	Blank contr. to $^{36}Ar_{prim}$	$(^{36}Ar/^{20}Ne)_{prim}$
K-DI-A3	0.316(5)	45(1)	1643(26)	3.51(8)	0.61(2)	5.33(4)	38(2)	1.1	16	1641(27)	0.0	43(2)
K-DI-A4	0.119(5)	43(2)	1619(68)	3.7(2)	0.71(5)	5.36(4)	35(3)	3.7	17	1620(69)	0.1	46(3)
K-DI-A5	0.170(5)	44(1)	1680(50)	3.5(1)	0.61(3)	5.37(4)	37(2)	2.1	15	1680(51)	0.0	45(2)
K-DI-A6	0.50(3)	45(3)	1660(100)	3.45(8)	0.62(2)	5.36(4)	38(3)	0.5	15	1658(100)	0.0	43(2)
K-DI-A7	0.616(5)	43.6(8)	1658(34)	3.6(1)	0.64(2)	5.4(1)	37(2)	0.5	15	1658(39)	0.0	45(2)
K-DI-A8	0.96(6)	42(3)	1596(104)	3.63(8)	0.64(2)	5.4(1)	36(3)	0.4	15	1598(106)	0.0	45(2)
K-DI-A9	1.31(3)	41(1)	1599(48)	3.73(6)	0.61(1)	5.4(1)	35(2)	0.3	15	1602(52)	0.0	46(2)
K-Ma-B	1.039(7)	13.8(3)	200(1)	1.51(4)	0.81(2)	5.21(5)	7.2(5)	1.0	48	199(2)	0.1	28(2)
K-Ma-C	0.737(7)	12.5(2)	143(1)	1.42(5)	0.80(3)	5.15(6)	6.2(5)	1.5	51	142(2)	0.1	23(2)
K-Rim-C	1.435(5)	9.5(1)	68.8(4)	1.26(2)	0.85(2)	4.96(4)	3.7(3)	5.7	61	68.0(5)	0.1	18(2)
K-Rim-H	0.27(1)	9.5(5)	60(3)	1.21(5)	0.87(4)	4.92(7)	3.3(6)	12.1	65	60(3)	1.8	18(3)

[a]Gas concentrations are given in units of (10^{-8} cm^3 STP/g). The correction of the measured ^{20}Ne and ^{36}Ar concentrations of cosmogenic contributions is explained in the text.

contribution (<2%) of cosmogenic Ar with a $^{36}Ar/^{38}Ar$ ratio of 0.65 (Table 1).

The blank contributions to the resulting $^{20}Ne_{prim}$ and $^{36}Ar_{prim}$ concentrations significantly increased only for those samples with relatively high cosmogenic contributions to the measured noble gas amounts (Tables 2–7). We exclude the possibility that the primordial component in our samples is compromised by adsorbed air to any significant degree. Our average primordial $^{20}Ne/^{22}Ne$ ratio of ~8.6 is in the range of HL gases (Fig. 5), distinctly below the air value of 9.8 (Table 1). Also, the $(^{36}Ar/^{20}Ne)_{prim}$ ratios (Tables 2–7) all lie significantly higher than the air ratio of 1.9 (Table 1) and are comparable to literature data of larger samples, as far as available. Most importantly, we are able to measure primordial gas concentrations, e.g., in chondrules, which are much smaller than the values reported for the gas-rich components here (e.g., Vogel 2003).

Calibrations

Sensitivity and mass discrimination of the spectrometer were determined by peak-height comparison using standard mixtures of high-purity Ne and Ar of roughly atmospheric isotopic composition in amounts believed to be known to within ~1% (Wieler et al. 1989). All isotopic ratios were corrected for mass discrimination. The corrections for Ne and Ar on the ion counting electron multiplier are ~0.2 and 0.8%/amu, respectively.

Uncertainties

All given uncertainties are 1σ. The reported uncertainties of the isotope concentration data (Tables 2–7) include statistical errors, uncertainties in sample weight, blanks, interferences, standard gas amounts, and, in the case of $^{20}Ne_{prim}$ and $^{36}Ar_{prim}$, uncertainties from the cosmogenic corrections. Uncertainties due to short-term variations in spectrometer sensitivity between sample and calibration analyses, which are ~1.5%, are not included. Inter-laboratory comparisons revealed a ~3% uncertainty in the determination of the absolute gas concentrations (Wieler et al. 1989). However, this does not affect the comparison of gas concentrations reported here. The uncertainties of the isotopic ratios (Tables 2–7) include statistical and blank uncertainties, as well as those from interference and mass discrimination corrections.

RESULTS

Isotopic Ratios

Neon

Figure 5 shows the Ne isotopic composition of all samples for Allende (a), Leoville (b), Renazzo (c), Semarkona (d), Bishunpur (e), and Krymka (f). In $^{20}Ne/^{22}Ne$ versus $^{21}Ne/^{22}Ne$

plots, the data points form mixing lines between the cosmogenic end members in the lower right and the primordial end members near the upper left corners. Regression of these mixing lines (taking into account uncertainties in [x] and [y] direction and forced through the respective cosmogenic end members) allows us to estimate the primordial $^{20}Ne/^{22}Ne$ ratios (numbers in boxes in Fig. 5) and, hence, the relative proportions of Ne-HL and Ne-Q for each meteorite. Due to the small database, we could not calculate single regressions for rims, matrix, and DIs of the respective meteorites. However, since most data points of each meteorite fall within uncertainties onto the respective mixing lines, similar mixing proportions of Ne-Q and Ne-HL in most samples within one meteorite can be assumed. Except for Krymka, all regressions lead to primordial $^{20}Ne/^{22}Ne$ ratios of 8.5–8.9, indicating that the Ne is mainly derived from presolar diamonds ($^{20}Ne/^{22}Ne$-HL 8.5, Table 1) with only small, if any, contributions of Ne-Q. This is in accordance with Huss and Lewis (1995) and Lewis et al. (1975) who show that primordial He and Ne in primitive meteorites are clearly dominated by the HL component with only a minor Q contribution.

The regression line through the Krymka samples yields a primordial $^{20}Ne/^{22}Ne$ ratio of 9.2 ± 0.2. This ratio is distinctly shifted toward Ne-Q ($^{20}Ne/^{22}Ne$ 10.1–10.7; Table 1), indicating some 15–60% of Ne-Q. The slope of the regression line is dominated by the data points of the Krymka DI, also showing an extraordinarily high $^{36}Ar_{prim}$ concentration (see below). Therefore, we assume that, mainly, the DI carries the unusual enrichment of Ne-Q.

Argon

Only ^{36}Ar and ^{38}Ar are useful to characterize different primordial noble gas reservoirs, since ^{40}Ar, in our samples, is mainly produced by the decay of radioactive ^{40}K. Furthermore, different trapped noble gas components show less variable $^{36}Ar/^{38}Ar$ than $^{20}Ne/^{22}Ne$ ratios. Only the $(^{36}Ar/^{38}Ar)_{HL}$ value of 4.41 and the cosmogenic component of ~0.65 are distinctly different from the $^{36}Ar/^{38}Ar$ ratios for Q, SW, and air, which all lie in the range of ~5.3 (Table 1). The relative cosmogenic contribution to the measured Ar is generally much lower than for Ne due to smaller cosmogenic production rates (e.g., Leya et al. 2000) and higher primordial Ar concentrations. Most of the samples show $^{36}Ar/^{38}Ar$ ratios around 5.2 (Tables 2–7), indicating that essentially all primordial Ar is derived from phase Q with only minor contributions of Ar-HL. This agrees with earlier reports showing that ~90% of the Ar in acid resistant residues resides in phase Q (e.g., Huss et al. 1996, and references therein). Only the Leoville DI and the Krymka rims K-Rim-C and K-Rim-H show slightly lower $^{36}Ar/^{38}Ar$ ratios of ~4.8. This can be attributed, in all probability, to the lower $^{36}Ar_{prim}$ concentrations in these samples compared to all other samples causing a relative increase of the respective cosmogenic ^{36}Ar-portion, and does not necessarily indicate the presence of significant amounts of Ar-HL. Since the exact primordial $^{36}Ar/^{38}Ar$ ratio for each meteorite hardly can be determined, we used the $(^{36}Ar/^{38}Ar)_Q$ ratio of Busemann et al. (2000) (Table 1) to correct all measured ^{36}Ar for cosmogenic contributions. Because this correction is very minor (0–2%), slightly variable primordial Ar compositions would hardly affect the inferred primordial ^{36}Ar concentrations.

Primordial Gas Concentrations and the Elemental Ratio $(^{36}Ar/^{20}Ne)_{prim}$

The $^{20}Ne_{prim}$ and $^{36}Ar_{prim}$ concentrations and $(^{36}Ar/^{20}Ne)_{prim}$ ratios of all samples (Tables 2–7) are presented in $(^{36}Ar/^{20}Ne)_{prim}$ versus $^{20}Ne_{prim}$ and $^{36}Ar_{prim}$ plots, respectively (Figs. 6–11). Two samples, L-Ma-C1 and L-Rim-C1, were discarded from the discussion due to substantial cross-contamination of rim and matrix material, which was already noted during the sample separation. However, for both samples pure aliquots exist. Two further samples, A-Rim-A1 and B-Rim-D, were discarded, since their $^{20}Ne_{prim}$ and/or $^{36}Ar_{prim}$ concentrations were in the range of the bulk values of the respective meteorites or were even distinctly lower. This indicates substantial contamination with chondrule material poor in primordial noble gases. Also, for A-Rim-A1, a pure aliquot existed. The discarded samples are shown in brackets in the plots and marked by italics in Tables 2–7.

Allende

Figure 6 shows the $(^{36}Ar/^{20}Ne)_{prim}$ ratios versus the $^{20}Ne_{prim}$ and $^{36}Ar_{prim}$ concentrations of rims (open circles), matrix (black solid circles), and DIs (grey triangles). The dark and light grey boxes comprise all matrix and rim data points, respectively. The presentation will be the same for all meteorites (Figs. 6–11). The box areas in Fig. 6 show a significant overlap in their primordial Ne and Ar concentrations and are identical within errors concerning their elemental ratios $(^{36}Ar/^{20}Ne)_{prim}$. All but one sample have $^{20}Ne_{prim}$ concentrations between 5×10^{-8} and ~8×10^{-8} cm^3 STP/g and $^{36}Ar_{prim}$ concentrations of 11×10^{-8} to 27×10^{-8} cm^3 STP/g. A-Rim-D (marked by arrows in Fig. 6), which was taken from a rim around an Allende CAI, is an exception with distinctly higher $^{20}Ne_{prim}$ and $^{36}Ar_{prim}$ concentrations, 13×10^{-8} and 41×10^{-8} cm^3 STP/g, respectively. The $(^{36}Ar/^{20}Ne)_{prim}$ for rims and matrix are identical within uncertainties and scatter between values of 3 and 4. Also, the 3 Allende DIs are within the range of $^{20}Ne_{prim}$ and $^{36}Ar_{prim}$ concentrations of rims and matrix. However, while A-DI-B and A-DI-C also show the same $(^{36}Ar/^{20}Ne)_{prim}$ ratios as rims and matrix, that of A-DI-B ($[^{36}Ar/^{20}Ne]_{prim}$ ~5) is the highest ratio of all Allende samples.

Leoville

Figure 7 shows that the Leoville rims contain distinctly higher $^{20}Ne_{prim}$ (29×10^{-8} to 34×10^{-8} cm^3 STP/g) and $^{36}Ar_{prim}$

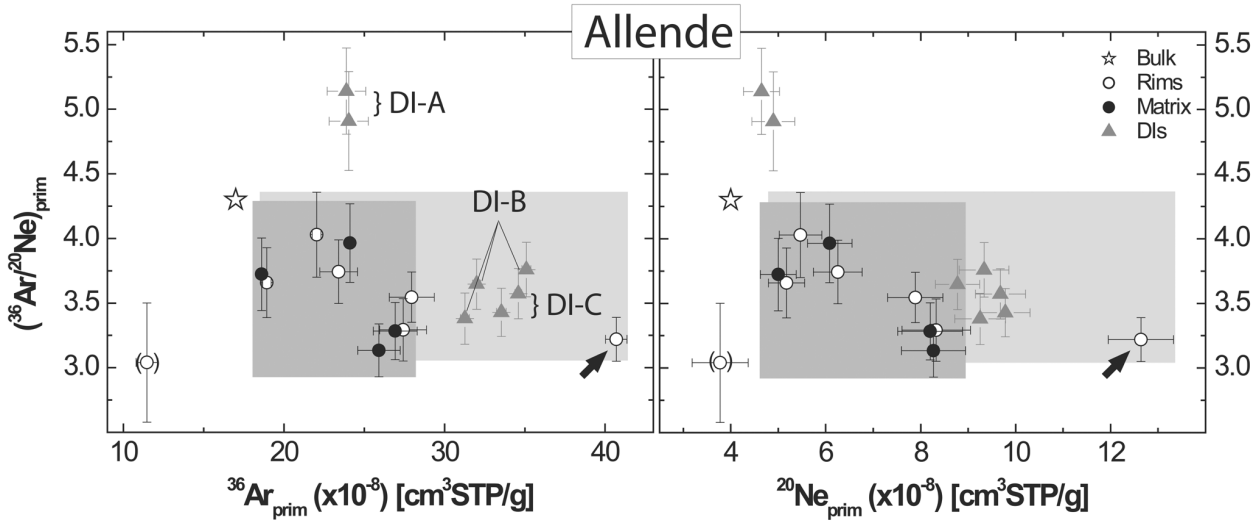

Fig. 6. $(^{36}Ar/^{20}Ne)_{prim}$ versus $^{36}Ar_{prim}$ and $^{20}Ne_{prim}$ of Allende rims, matrix, and DIs, respectively. The star symbols represent average bulk data (Schultz and Franke 2000). The discarded data points are in brackets. The light grey and grey boxes contain all rim and all matrix samples, respectively. See the text for further explanations.

(650 × 10^{-8} to 813 × 10^{-8} cm^3 STP/g) concentrations than the matrix ($^{20}Ne_{prim}$: 12 × 10^{-8} to 29 × 10^{-8} cm^3 STP/g; $^{36}Ar_{prim}$: 311 × 10^{-8} to 580 × 10^{-8} cm^3 STP/g), not taking into account the discarded samples. The $(^{36}Ar/^{20}Ne)_{prim}$ ratios between 22 and 27 are identical within errors for rims and matrix. The Leoville DI (marked by arrows in Fig. 7) shows the lowest primordial gas concentrations of all Leoville samples. Its $^{20}Ne_{prim}$ is ~2 times, and the $^{36}Ar_{prim}$ 24 times, lower than the respective matrix value. Therefore, the $(^{36}Ar/^{20}Ne)_{prim}$ ratio of the DI of ~2.5 is roughly one order of magnitude lower than the average $(^{36}Ar/^{20}Ne)_{prim}$ ratio of the matrix.

Renazzo

The Renazzo rims (Fig. 8) show clearly lower $^{36}Ar_{prim}$ concentrations between 50 × 10^{-8} and 64 × 10^{-8} cm^3 STP/g than the matrix with 72 × 10^{-8} to 91 × 10^{-8} cm^3 STP/g. Also, the $^{20}Ne_{prim}$ concentrations tend to be lower for the rims (13 × 10^{-8} to 16 × 10^{-8} cm^3 STP/g) than for the matrix (16 × 10^{-8} to 23 × 10^{-8} cm^3 STP/g). However, a significant overlap between the 2 boxes—taking in account the uncertainties—exists for the $^{20}Ne_{prim}$. This is probably due to the higher uncertainty of the correction for cosmogenic Ne compared to the Ar. The $(^{36}Ar/^{20}Ne)_{prim}$ ratios are identical for rims and matrix, scattering around a value of ~4.

Semarkona

Figure 9 shows that the Semarkona rims contain, on average, twice as high $^{20}Ne_{prim}$ and $^{36}Ar_{prim}$ concentrations than the matrix. The rims have $^{20}Ne_{prim}$ concentrations of 20 × 10^{-8} to 24 × 10^{-8} cm^3 STP/g and $^{36}Ar_{prim}$ concentrations between 266 × 10^{-8} and 361 × 10^{-8} cm^3 STP/g. The matrix has $^{20}Ne_{prim}$ concentrations of 10 × 10^{-8} to 15 × 10^{-8} cm^3 STP/g and $^{36}Ar_{prim}$ concentrations between 131 × 10^{-8} and 221 × 10^{-8} cm^3 STP/g. The $(^{36}Ar/^{20}Ne)_{prim}$ ratios scatter around 14 and are identical within uncertainties for rims and matrix.

Bishunpur

The Bishunpur matrix in Fig. 10 shows $^{20}Ne_{prim}$ concentrations between 4 × 10^{-8} and 6 × 10^{-8} cm^3 STP/g and $^{36}Ar_{prim}$ concentrations between 85 × 10^{-8} and 143 × 10^{-8} cm^3 STP/g. The two rim samples have very different noble gas signatures: B-Rim-G shows higher $^{20}Ne_{prim}$ and $^{36}Ar_{prim}$ concentrations than the matrix, 8 × 10^{-8} and 183 × 10^{-8} cm^3 STP/g, respectively. In contrast, B-Rim-D has a primordial noble gas signature in the range of Bishunpur bulk. This indicates a substantial contamination of this sample with noble gas-poor chondrule material and led us to discard the sample. In contrast to Leoville, we do not have independent evidence for the contamination. Nevertheless, without taking into account the B-Rim-D sample, the Bishunpur rim has higher $^{20}Ne_{prim}$ and $^{36}Ar_{prim}$ concentrations than the matrix, while no differences in the $(^{36}Ar/^{20}Ne)_{prim}$ ratios of rims and matrix (scattering between 19 and 23) are visible.

Krymka

The Krymka rims show distinctly lower $^{20}Ne_{prim}$ (3 × 10^{-8} to 4 × 10^{-8} cm^3 STP/g) and $^{36}Ar_{prim}$ (60 × 10^{-8} to 68 × 10^{-8} cm^3 STP/g) concentrations than the matrix (Fig. 11). The matrix contains 6 × 10^{-8} to 7 × 10^{-7} cm^3 STP/g $^{20}Ne_{prim}$ and 142 × 10^{-8} to 199 × 10^{-8} cm^3 STP/g $^{36}Ar_{prim}$. Also, the $(^{36}Ar/^{20}Ne)_{prim}$ ratios are smaller for the rims than for the matrix. Taking into account the respective uncertainties, the $(^{36}Ar/^{20}Ne)_{prim}$ ratios of the rims range from 15–21, and those of the matrix range from 21 to 30.

The Krymka DI (Fig. 4) shows the highest primordial noble gas concentrations of all samples presented here with

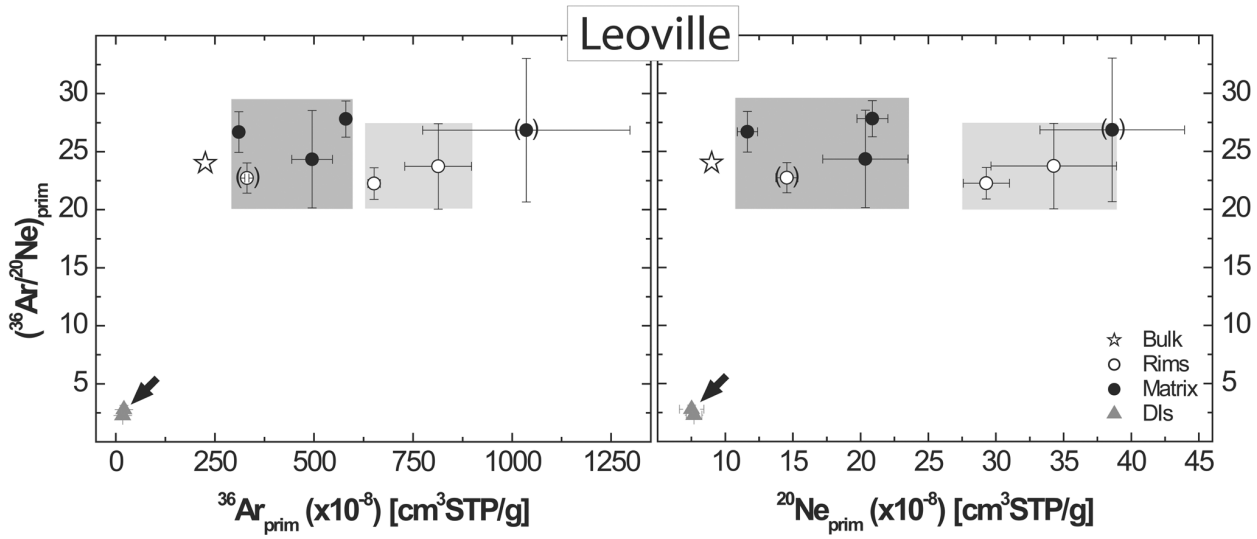

Fig. 7. $(^{36}Ar/^{20}Ne)_{prim}$ versus $^{36}Ar_{prim}$ and $^{20}Ne_{prim}$ of Leoville rims, matrix, and DIs, respectively. The star symbols represent average bulk data (Schultz and Franke 2000). The discarded data points are in brackets. The light grey and grey boxes contain all rim and all matrix samples, respectively. See the text for further explanations.

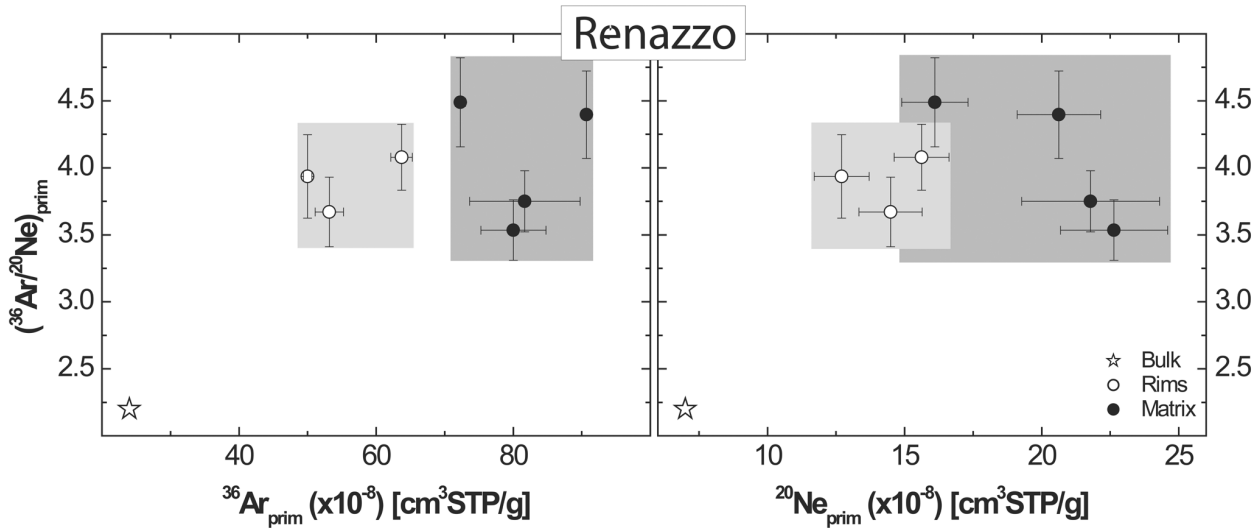

Fig. 8. $(^{36}Ar/^{20}Ne)_{prim}$ versus $^{36}Ar_{prim}$ and $^{20}Ne_{prim}$ of Renazzo rims and matrix, respectively. The star symbols represent average bulk data (Schultz and Franke 2000). The light grey and grey boxes contain all rim and all matrix samples, respectively. See the text for further explanations.

~37 × 10^{-8} cm^3 STP/g $^{20}Ne_{prim}$ and even ~1637 × 10^{-8} cm^3 STP/g $^{36}Ar_{prim}$. The $^{36}Ar_{prim}$ is enriched relative to the matrix by an order of magnitude and is comparable to $^{36}Ar_{prim}$ concentrations in bulk acid resistant residues, where the carrier phase Q has been chemically enriched (e.g., Busemann et al. 2000). Its $(^{36}Ar/^{20}Ne)_{prim}$ ratio of ~45 is the highest of all $(^{36}Ar/^{20}Ne)_{prim}$ ratios in this study.

DISCUSSION

In the previous sections, we have shown that the Ne isotopic composition of nearly all samples is dominated by Ne-HL. Only the Krymka DI shows a significant contribution of Ne-Q. The Ar isotopic signature is always dominated by Ar of phase Q. Clear differences in the $^{20}Ne_{prim}$ and $^{36}Ar_{prim}$ concentrations between rims and matrices could be detected for Semarkona, Krymka, and Renazzo (here mainly in the $^{36}Ar_{prim}$ concentration). Apart from the few discarded samples discussed in the Results section, the same is basically true for Leoville and Bishunpur rims and matrices. Allende rims and matrix show uniform $^{20}Ne_{prim}$ and $^{36}Ar_{prim}$ concentrations except for A-Rim-D, which has distinctly higher primordial Ne and Ar concentrations. Except for Krymka, the $(^{36}Ar/^{20}Ne)_{prim}$ ratios of rims and matrices in the respective meteorites are

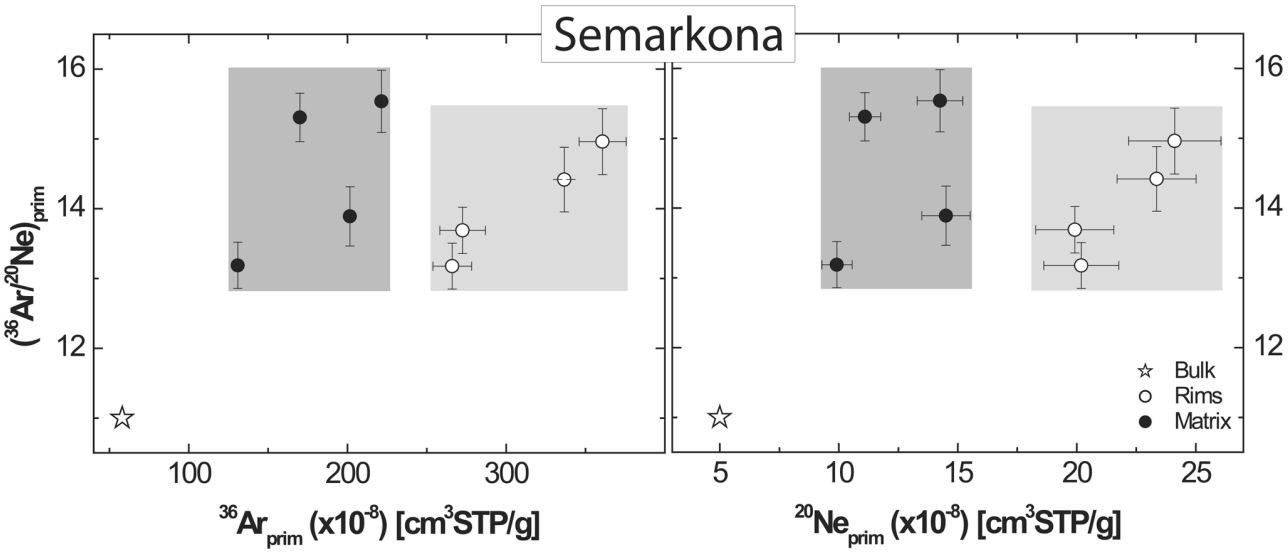

Fig. 9. $(^{36}Ar/^{20}Ne)_{prim}$ versus $^{36}Ar_{prim}$ and $^{20}Ne_{prim}$ of Semarkona rims and matrix, respectively. The star symbols represent average bulk data (Schultz and Franke 2000). The light grey and grey boxes contain all rim and all matrix samples, respectively. See the text for further explanations.

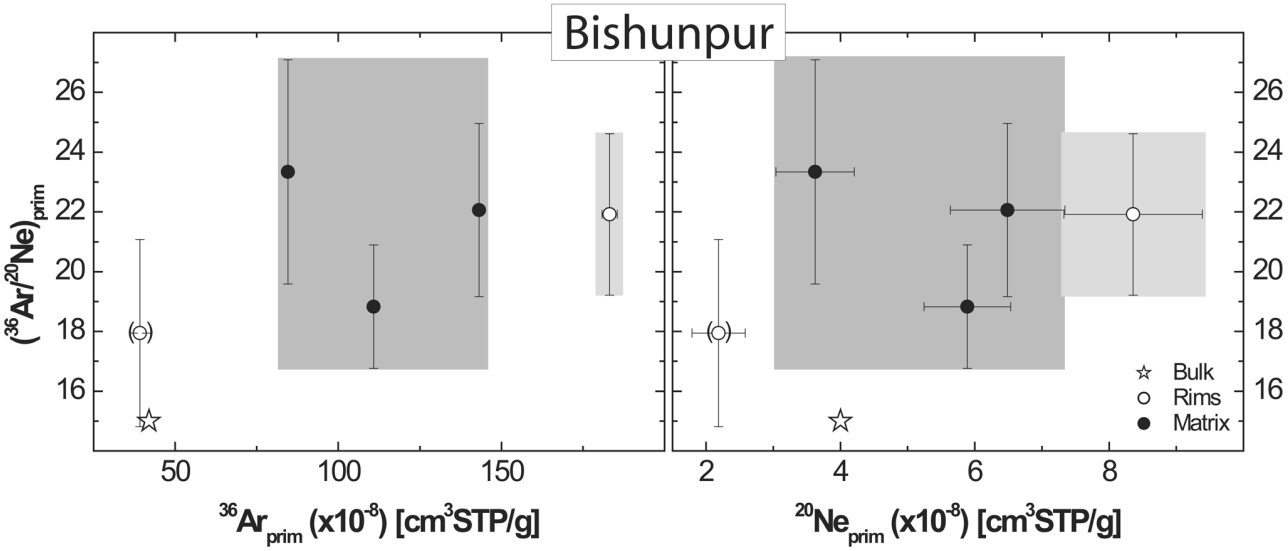

Fig. 10. $(^{36}Ar/^{20}Ne)_{prim}$ versus $^{36}Ar_{prim}$ and $^{20}Ne_{prim}$ of Bishunpur rims and matrix, respectively. The star symbols represent average bulk data (Schultz and Franke 2000). The light grey and grey boxes contain all rim and all matrix samples, respectively. Most probably due to contamination with chondrule material, one rim sample (in brackets) lies in the range of bulk ^{36}Ar and ^{20}Ne concentrations. See the text for further explanations.

identical within uncertainties. The Leoville and Krymka DIs and one of the Allende DIs (A-DI-A) display noble gas signatures different from their respective host rim and matrix material.

Relationship Between Rims and Matrix

Formation Models of Rims and Matrix

Basically, two contrasting ideas about rim formation have been discussed in the literature. These are: 1) rim formation by various processes on parent bodies, and 2) rim formation by accretion in the nebula. After a brief introduction of some models, we will discuss these ideas in the context of our noble gas data for rims and matrices.

In the framework of rim formation on parent bodies, Sears et al. (1991, 1993) suggested that chondrule rims of the CM chondrite Murchison were formed by aqueous alteration of the host chondrule material in situ. Bunch et al. (1991) postulated the formation of granular and opaque rims around chondrules in some OCs during impact processes partly

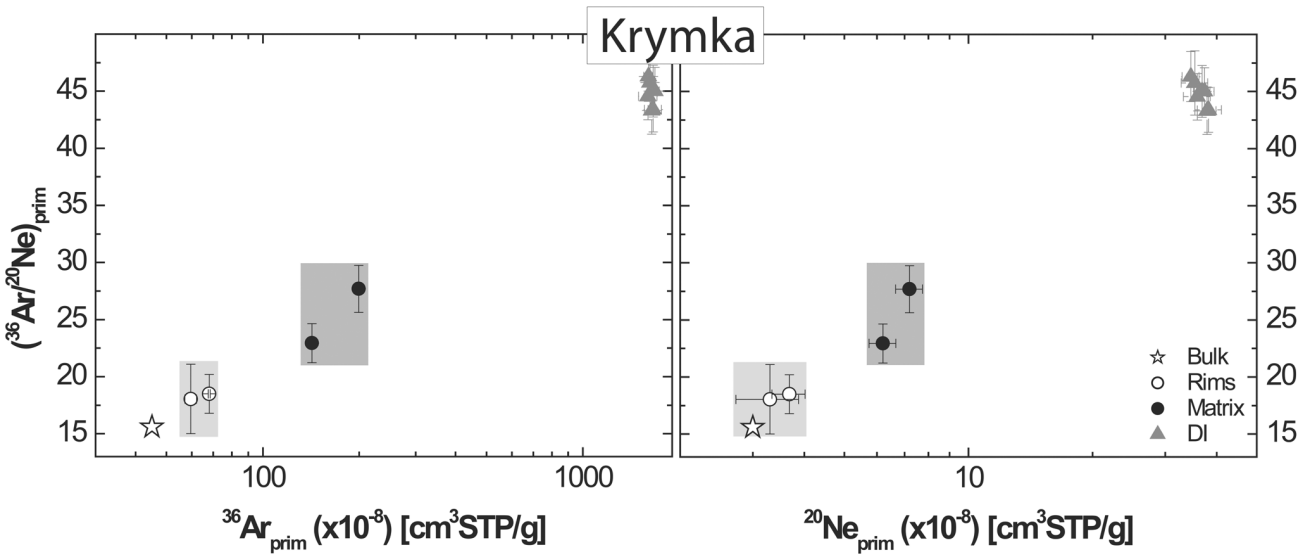

Fig. 11. $(^{36}Ar/^{20}Ne)_{prim}$ versus $^{36}Ar_{prim}$ and $^{20}Ne_{prim}$ of Krymka rims, matrix, and DIs, respectively. The star symbols represent average bulk data (Schultz and Franke 2000). The light grey and grey boxes contain all rim and all matrix samples, respectively. Note the logarithmic scale of the x-axis. See the text for further explanations.

accompanied by melting and fragmentation of the outer margins of the host chondrules. Tomeoka and Tanimura (2000) proposed the formation of phyllosilicate-rich chondrule rims in the CV chondrite Vigarano by aqueous alteration of matrix around chondrules on the Vigarano parent body. Subsequently, the rock was brecciated and clasts composed of one chondrule plus surrounding matrix were rounded. The rounded clasts were finally transported to anhydrous regions of the Vigarano regolith.

"Nebular models" postulate the sticking of fine-grained dust to the surfaces of chondrules and other objects to form accretionary rims in the solar nebula before these rimmed objects were incorporated into parent bodies (e.g., Hua et al. 2002; Metzler and Bischoff 1996; Metzler et al. 1992, and references therein; Nakamura et al. 1999b). Nakamura et al. (1999b), who found that the rim component for 2 CM chondrites contained the highest primordial noble gas concentrations, also postulate an accretionary origin for these rims. MacPherson et al. (1985) conclude that rims and matrix in Allende reflect time-dependent nebular accretion sequences, with the rims being accreted before the matrix.

Behavior of Primordial Noble Gases During Alteration Processes

The abundance of primordial noble gases in different types of chondrites decreases with increasing metamorphic grade (Heymann and Mazor 1968; Huss et al. 1996; Marti 1967; Sears et al. 1980). Furthermore, Huss et al. (1996) found that, in unequilibrated ordinary chondrites, the abundance of Q-gases ("P1" in their notation) decreased more slowly with increasing petrographic subtype than the abundance of HL-gases from presolar grains. Semarkona, Bishunpur, and Krymka were among the meteorites studied by these authors and are also investigated here. Huss and coworkers concluded that the Q-carrier in unequilibrated ordinary chondrites is more resistant to metamorphism than the HL-carrying presolar diamonds. Nakamura et al. (1999a) reported an inverse correlation of the abundance of heavy primordial noble gases and the degree of hydrothermal alteration in CM chondrites. In accordance with these results, laboratory experiments by Nakasyo et al. (2000) found that artificial hydrothermal alteration of the CV chondrite Allende led to a decrease of the primordial noble gas concentration in the sample. In particular, the authors found that Xe-HL was lost more easily than Xe-Q, and concluded that the HL-carrier is probably less resistant to hydrothermal alteration than phase Q. The above results indicate that thermal and hydrothermal alteration have a similar effect on the primordial noble gas inventory in different chondrite classes, i.e., not only a general decrease of the primordial noble gas concentrations but also a more pronounced loss of noble gases from presolar diamonds than from phase Q.

Since the $^{20}Ne_{prim}$ of our samples is dominated by HL-gases and the $^{36}Ar_{prim}$ is predominantly carried by phase Q, based on the above observations, we expect that thermal or hydrothermal alteration leads to a decrease of the primordial noble gas concentrations and probably a simultaneous increase of the $(^{36}Ar/^{20}Ne)_{prim}$ ratio due to the preferential susceptibility of the Ne-carrying presolar diamonds to alteration.

Formation of Rims by Alteration Processes?

Formation of rims by aqueous alteration of matrix on a parent body, as proposed by Tomeoka and Tanimura (2000),

should result in lower primordial noble gas concentrations and—based on the observations outlined above—presumably higher $(^{36}Ar/^{20}Ne)_{prim}$ ratios in the rims than in the matrix. In the case of rim formation from chondrules, which contain only very low primordial noble gas concentrations (e.g., Nakamura et al. 1999b; Vogel 2003), the rims should contain substantially lower primordial noble gas concentrations than the matrix. Further, the rims might well be expected to also have lower $(^{36}Ar/^{20}Ne)_{prim}$ ratios than the matrix, since chondrules may have distinctly lower $(^{36}Ar/^{20}Ne)_{prim}$ ratios than the surrounding matrix (e.g., Vogel 2003).

Regarding the primordial noble gas concentrations, neither the $^{20}Ne_{prim}$ nor the $^{36}Ar_{prim}$ concentrations of Allende, Leoville, Semarkona, and Bishunpur decrease from matrices to rims. For these samples, rim formation by aqueous alteration of matrix in a parent body environment is, therefore, excluded. In contrast, Renazzo and Krymka rims have lower primordial Ne and Ar concentrations than the respective matrices. Thus, in these cases, rim formation by alteration of matrix would be possible in principle. However, Renazzo rims and matrix show identical $(^{36}Ar/^{20}Ne)_{prim}$ ratios, which is not predicted by the particular alteration systematics described above. In fact, quite possibly, the differences in the $(^{36}Ar/^{20}Ne)_{prim}$ ratios between rims and matrix are small and, thus, remain undetected due to the relatively large uncertainties of these ratios. The Krymka rims with lower primordial noble gas concentrations and lower $(^{36}Ar/^{20}Ne)_{prim}$ ratios than the matrix, could theoretically point to a rim formation by alteration of chondrule margins. However, the $^{36}Ar_{prim}$ concentrations of the rims, especially, are distinctly too high to be formed from chondrules (compare, e.g., Vogel [2003]). Taking into account, also, the noble gas signature of the Krymka DI, a nebular formation scenario can most consistently explain the noble gas signatures of the Krymka rims and matrix (see below).

Nebular Formation of Rims and Matrix?

In the context of nebular rim and matrix formation, the noble gas carriers would have accreted together with the fine-grained silicate dust onto chondrules and other objects before the latter were incorporated into a parent body. The decrease of primordial noble gas concentrations from earlier accreted rims to later accreted matrix could then reflect a time-dependent decrease of the primordial noble gas abundance in the nebular reservoir from which accretion took place. Several possible scenarios could explain such a decrease:

1. Thermal or aqueous alteration of the nebular dust itself (e.g., Metzler et al. 1992, and references therein) could lead to a progressive decrease of its primordial noble gas concentrations. The nebular $(^{36}Ar/^{20}Ne)_{prim}$ ratio might show a slight simultaneous increase due to the preferential attack of the Ne carrier during alteration.
2. Dilution of the noble gas carrying dust with noble gas-poor chondrule debris would lead to a decrease of the primordial noble gas concentrations in the nebula. Also, the nebular $(^{36}Ar/^{20}Ne)_{prim}$ ratios are expected to slightly decrease due to the low $(^{36}Ar/^{20}Ne)_{prim}$ ratios found in chondrules (e.g., Vogel 2003). Variable amounts of chondrule debris are well-known to be present in the matrix-like portions of unequilibrated chondrites (Alexander 1989; Brearley 1996), and, e.g., Housley and Cirlin (1983) suggested that the Allende matrix is predominantly composed of altered chondrule material.
3. Finally, we discuss the possibility of a dilution of phase Q and the presolar diamonds by subsequently condensing (essentially noble gas-free) nebular dust, based on the following arguments.

Phase Q and presolar diamonds in primitive chondrites are homogeneously mixed on a μm-scale (e.g., Huss and Alexander 1987; Huss et al. 1996; Nakamura et al. 1999b; Amari et al. 2001). Huss and Alexander (1987) and Huss et al. (1996), therefore, postulate a presolar origin also for phase Q or, at least, a thorough mixing of phase Q and the presolar diamonds very early in the solar nebula. Supporting evidence for a presolar origin of phase Q comes from experiments that successfully trap heavy noble gases on carbonaceous materials under interstellar molecular cloud conditions (Sandford et al. 1998). Also, Busemann et al. (2001) postulate that both carrier phases must have been thoroughly mixed before the onset of planetesimal accretion. Naturally, one would assume that if the presolar grains and phase Q were present very early in the solar nebula, they were also avaibable for early incorporation into accreting material. In line with this assumption, Nakamura et al. (1999b) conclude, from studying noble gases in fine-grained rims around chondrules in CM chondrites, that the presolar diamonds were homogeneously mixed to the accretion region of these rims already at a very early stage of solar system evolution.

Based on the above reasoning, we argue that subsequently condensing nebular dust (essentially free of primordial noble gases) might have progressively diluted the primordial noble gas concentrations (i.e., their carrier phases) in a given nebular reservoir without changing the $(^{36}Ar/^{20}Ne)_{prim}$ ratio.

The primordial noble gas concentrations decrease from rims to matrix in Leoville, Semarkona, and Bishunpur, which indicates a nebular rim and matrix formation. This is in accordance with the results of MacPherson et al. (1985), Metzler and Bischoff (1996), and Metzler et al. (1992), who propose rim and matrix formation by progressive accretion from slightly changing dust reservoirs. No systematic differences in the $(^{36}Ar/^{20}Ne)_{prim}$ ratios between rims and matrix could be detected. Therefore, the third scenario, dilution by condensing material, would best match our results. However, the second conclusion is not unambiguous, since, again, possible systematic variations of the $(^{36}Ar/^{20}Ne)_{prim}$ ratios between rims and matrix might be smaller than the uncertainties of the respective $(^{36}Ar/^{20}Ne)_{prim}$ ratios.

Allende rims and matrix, basically, do not show differences in their primordial noble gas signatures. However, the exceptional A-Rim-D shows nearly twice as high $^{20}Ne_{prim}$ and $^{36}Ar_{prim}$ concentrations than the other rim and matrix samples, associated with a similar $(^{36}Ar/^{20}Ne)_{prim}$ ratio. For this rim, the third nebular scenario would, in principal, match Leoville, Bishunpur, and Semarkona. We suggest that the time span between the accretion of the other Allende rims and the matrix was too short to establish any detectable differences in their noble gas signatures. In contrast, the CAI could have achieved its accretionary rim somewhat earlier from a slightly differing reservoir.

Alternative Formation Scenarios for Krymka and Renazzo Rims and Matrices

The primordial noble gas concentrations increase from Krymka and Renazzo rims to matrices, respectively. For Krymka, this is accompanied by an increase of the $(^{36}Ar/^{20}Ne)_{prim}$ ratios. None of the alteration scenarios consistently explains the Krymka noble gas signatures. However, the data can be explained by a progressive admixture of material with high primordial noble gas concentrations and high $(^{36}Ar/^{20}Ne)_{prim}$ ratios to the nebular region, from which first the rims and then the matrix accreted. Evidence for the presence of such material in the Krymka accretion region is provided by the Krymka DI, which matches exactly the requirements stated above. Another Krymka DI with a similar noble gas inventory had already been reported by Lewis et al. (1979), showing that the Krymka parent body trapped more material with noble gas signatures very different from those of Krymka rims and matrix. Just about 7% of DI-like dust admixed to the rim material could explain the $^{20}Ne_{prim}$ and $^{36}Ar_{prim}$ concentrations of the Krymka matrix. Thus, we suggest that after the accretion of fine-grained rims on Krymka chondrules, material from a different region with a noble gas signature similar to that of the Krymka DI was admixed to the original dust reservoir. The added dust led to increasing primordial noble gas concentrations and $(^{36}Ar/^{20}Ne)_{prim}$ ratios of the progressively accreting Krymka matrix. Macroscopic clasts of the added material represent the present-day DIs in Krymka.

The higher primordial gas concentrations of the Krymka matrix samples are highly unlikely to be an artifact due to admixture of DI-dust during sawing and polishing of the sample chip. First, the amount of 7% of DI-admixture to the matrix samples is very high taking into account that the DI occupies less than 5% of the overall surface area of the sample chip. Second, in this case, we would not expect the clear difference between rim and matrix noble gas patterns, but, rather, homogeneous noble gas patterns for all rim and matrix samples.

The increase of the $^{20}Ne_{prim}$ and $^{36}Ar_{prim}$ from Renazzo rims to matrix could be explained by a formation of the rims by alteration of matrix as stated above. However, taking into account the data of Krymka, also an admixture of noble-gas-rich material to a reservoir from which first rims and subsequently matrix accreted to the Renazzo parent body would lead to the observed noble gas concentrations. In fact, we do not have particular evidence for the presence of a gas-rich component in the case of Renazzo as we do for Krymka. The Renazzo noble gas data do not allow a final conclusion about the formation of its rims and matrix, either by aqueous alteration or by nebular mixing processes.

Relationship Between Dark Inclusions and Rims and Matrix

Studies of dark inclusions in chondrites revealed a considerable diversity in their textures, indicating multiple sources and/or complex formation or alteration histories of the DIs (Brearley and Jones 1998). Most formation scenarios for DIs include the accretion of nebular dust to small or larger precursor bodies. Subsequently, these bodies are destroyed or single fragments of them are released by impacts to the nebular reservoir, from where the final accretion of the mm- to cm-sized objects to the present-day host meteorites took place (Bischoff 1989; Bischoff et al. 1988; Grady et al. 1999; Johnson et al. 1990; Kurat et al. 1989; Semenenko et al. 2001). The degrees of precursor body, nebular, and parent body alteration of the DIs are highly variable in these scenarios (e.g., Buchanan et al. 1996; Kojima and Tomeoka 1997; Tomeoka and Kojima 1998).

Based on mineralogical observations, Semenenko et al. (2001) describe in detail the evolution of the Krymka dark inclusion "fragment BK13," which is from the same DI as the Krymka DI studied here: dust particles first accreted to small porous spherules and then to fine-grained "accretionary rocks." After mild thermal metamorphism, these were destroyed by impacts, and the fragments were transported into the nebular formation region of Krymka where they were admixed to the Krymka host meteorite.

Of each studied DI, at least 2 noble gas measurements exist, which mostly are identical within uncertainties (see Figs. 6, 7, and 11). This shows that the primordial noble gases are distributed relatively homogeneously throughout the respective DIs. Differences in the noble gas signatures of different DIs, thus, cannot be attributed to biased sampling.

The Allende DIs A-DI-B and A-DI-C are similar to each other and to Allende rims and matrix in their primordial Ne and Ar concentrations and $(^{36}Ar/^{20}Ne)_{prim}$ ratios. In contrast, A-DI-A contains less $^{20}Ne_{prim}$ and $^{36}Ar_{prim}$ and a higher $(^{36}Ar/^{20}Ne)_{prim}$ ratio than the other DIs. This indicates a higher degree of alteration of A-DI-A compared to A-DI-B and A-DI-C. Since all studied Allende DIs were located within an area of ~10 × 10 cm^2, parent body alteration in their final location should have affected all of them in a similar way. Therefore, A-DI-A likely obtained the differing noble gas signature due to a higher degree of alteration

before it was incorporated at its final location in the Allende parent body. The more gas-rich DIs A-DI-B and A-DI-C may have formed by accretion of small chunks of dusty material from the same nebular region and simultaneously to Allende rims and matrix. Also, they might represent fragments of Allende itself, released and redistributed during smaller impact events on the Allende parent body. The altered A-DI-A, instead, could represent a fragment from a larger hydrous precursor body that accreted in the same nebular region as Allende or from a distant water-rich region of the Allende parent body itself, from where fragments were redistributed to their present locations by impacts, as proposed, e.g., by Johnson et al. (1990).

The Leoville DI shows by far the lowest noble gas concentrations of all Leoville components studied here, with a $(^{36}Ar/^{20}Ne)_{prim}$ ratio one order of magnitude lower than the rim and matrix values. As outlined above, we assume that a decrease of the noble gas concentrations by thermal or hydrothermal alteration is generally accompanied by an increase of the $(^{36}Ar/^{20}Ne)_{prim}$ ratio. Thus, we cannot explain the noble gas signature of the DI as an alteration product from the same material as the Leoville rims and matrix. In agreement with Kracher et al. (1982), we propose that this clast originated from a different precursor with the required noble gas signatures and was later added to the Leoville parent body.

The Krymka DI contains extraordinarily high primordial noble gas concentrations and also the highest elemental ratio $(^{36}Ar/^{20}Ne)_{prim}$ of all our samples. Since we cannot conceive of a secondary process that would increase the primordial noble gas concentration in a fine-grained low-temperature object, we exclude the possibility that Krymka rims and matrix are a precursor material for the DI. On the other hand, a decrease of the primordial noble gas concentrations by alteration should be accompanied by an increasing $(^{36}Ar/^{20}Ne)_{prim}$ ratio as stated above. Thus, the DI cannot have served as a precursor material for Krymka rims and matrix either. In agreement with Semenenko et al. (2001), we conclude that the Krykma DI ("BK 13") originated from a different precursor, which accreted in a region with distinctly different noble gas signatures than the one that delivered Krymka rims and matrix. Further evidence for such a "Krymka DI precursor rock" is provided by a trace element and noble gas study on another DI in Krymka (Lewis et al. 1979). This sample also has a relatively high $^{20}Ne/^{22}Ne$ of ~9.1, contains even more $^{20}Ne_{prim}$ than ours, and has a lower $(^{36}Ar/^{20}Ne)_{prim}$ ratio of ~15. Compared to the DI of Lewis et al. (1979), ours has probably experienced a slightly higher degree of thermal or hydrothermal alteration lowering the $^{20}Ne_{prim}$ concentrations in particular and, thus, increasing the $(^{36}Ar/^{20}Ne)_{prim}$ ratio. Low temperature processing of our DI before its incorporation to the Krymka parent body was also concluded by Semenenko et al. (2001). Despite slightly different alteration states, the extraordinarily high gas concentrations in both DIs argue for a common origin. Lewis et al. (1979) concluded that their DI represented a late condensate that collected large amounts of volatiles like Ag, Bi, and Tl left behind by earlier generations of meteorites, forming a primitive C-chondritic body. This is in contrast to Semenenko and coworkers concluding that their DI (also studied by us) has retained the record of the first stages of accretion of cosmic material, possibly even before the onset of chondrule formation. Furthermore, accretion, variable alteration, and disruption of the DI precursor body must have predated the formation of the Krymka parent body, which also requires an early accretion of the DI material. Considering this, we conclude that high amounts of phase Q and presolar diamonds must have been available for accretion at a very early stage of solar system evolution.

In summary, the Allende DIs probably accreted from the same region as Allende rims and matrix, but A-DI-A, especially, suffered a higher degree of alteration than the others. In contrast, the DIs of Leoville and Krymka have noble gas signatures differing substantially from those of their respective host meteorites, indicating an accretion from different regions in the solar nebula, respectively. Thus, the nebular reservoir in the accretion area of the meteorites must have been heterogeneous on a large scale with respect to the noble gas signatures. However, we agree with Nakamura et al. (1999b) that, on a small scale (e.g., within one DI), phase Q and the presolar diamonds seem to be well-mixed. Individual present-day chondrites must have sampled material from different regions in continuously changing proportions.

CONCLUSIONS

In this study, we used the primordial ^{20}Ne and ^{36}Ar signatures of fine-grained rims, matrices, and dark inclusions of 6 type 2 and 3 chondrites to reveal genetic relationships among these components and draw conclusions on accretionary and alteration processes in the solar nebula. Differences of the $^{20}Ne_{prim}$ and $^{36}Ar_{prim}$ concentrations between rims and matrices could be detected in most meteorites, although, in the case of Allende, only for one rim sample. The differing noble gas signatures can be explained mostly in the framework of a time-dependent nebular accretion sequence of rims and, subsequently, matrix.

The rims of Semarkona and—with restrictions due to cross-contamination of some samples—also of Leoville and Bishunpur contain higher primordial Ne and Ar concentrations than the respective matrices, but similar $(^{36}Ar/^{20}Ne)_{prim}$ ratios. This is explained by a progressive accretion of fine-grained nebular dust from a reservoir with decreasing primordial noble gas content. The decrease is most probably due to a continuous dilution of the carrier phases of HL- and Q-gases with essentially noble gas-free condensing material. However, also an admixture of chondrule debris is possible. Underlying is the assumption that both phase Q and the

presolar diamonds were available for accretion at a very early stage of solar system evolution. Most of the Allende rims and the matrix seem to have accreted very fast to the Allende parent body so that no measurable differences in the noble gas signatures of rims and matrix could be established. Only one Allende rim enclosing a CAI shows distinctly higher primordial Ne and Ar concentrations than the other Allende samples. It seems to have accreted to the CAI somewhat earlier from a slightly different reservoir.

The primordial Ne and Ar concentrations and the $(^{36}Ar/^{20}Ne)_{prim}$ ratio of Krymka increase from rims to matrix, indicating an admixture of primordial noble gas-rich dust to the region, from which Krymka rims and then matrix progressively accreted. Larger clasts of the gas-rich material were incorporated as DIs into the Krymka parent body.

Renazzo also shows higher primordial Ne and Ar concentrations in the matrix than in the rims but similar $(^{36}Ar/^{20}Ne)_{prim}$ ratios. This could be explained either by formation of the rims from matrix by alteration processes or, similar to Krymka, by admixture of dust with higher primordial noble gas concentrations to the reservoir, from which rims and, subsequently, the matrix accreted to the Renazzo parent body.

The Allende DIs probably accreted from the same nebular region as Allende rims and matrix, but one DI suffered a higher degree of alteration before it was incorporated into its final location in the parent body. The DIs of Leoville and Krymka have noble gas signatures very different from those of their respective host meteorites, indicating accretion from different nebular regions than their respective rims and matrices.

Our noble gas data imply a heterogeneous dust reservoir in the accretion region of the meteorites. This is not only due to the different noble gas signatures among the different meteorites studied but also because of the differences of the noble gas signatures among the different fine-grained constituents within one meteorite. Further studies are needed to decide whether the heterogeneity of the nebula is primarily due to variable mixing of the primordial noble gas carrier phases of HL- and Q-gases with primordial noble gas-free matter. Alternatively, an originally uniform noble gas signature of the solar dust reservoir could have been fractionated later to various degrees in different regions of the solar nebula.

Acknowledgments–We are grateful to I. Lyon, A. Patzer, and an anonymous reviewer, whose thorough reviews considerably improved the quality of the manuscript. We further thank H. Busemann for a very helpful informal review of the manuscript. We thank the Muséum National d'Histoire Naturelle (Paris) and the Smithsonian National Museum of Natural History (Washington, DC) for providing samples of Renazzo and Semarkona (USNM 1805), respectively. We further thank the Natural History Museum (London) and the SSC of Environmental Radiochemistry (Kyiv) for providing samples of Bishunpur and Krymka, respectively. For assistance with SEM work, we are grateful to T. Grund, A. Baarnholm, and K. Kunze. This work was supported by the Swiss National Science Foundation.

Editorial Handling— Dr. Ian Lyon

REFERENCES

Alexander C. M. O. 1989. Origin of chondrule rims and interchondrule matrices in unequilibrated ordinary chondrites. *Earth and Planetary Science Letters* 95:187–207.

Amari S., Zaizen S., Matsuda J. 2001. Search for Q (abstract). *Meteoritics & Planetary Science* 36:A10–A11.

Anders E. and Zinner E. 1993. Interstellar grains in primitive meteorites: Diamond, silicon carbide, and graphite. *Meteoritics & Planetary Science* 28:490–514.

Benkert J., Baur H., Signer P., and Wieler R. 1993. He, Ne, and Ar from the solar wind and solar energetic particles in lunar ilmenites and pyroxenes. *Journal of Geophysical Research* 98: 13147–13162.

Bischoff A. 1989. Mineralogische und chemische Untersuchungen an chondritischen Meteoriten: Folgerungen für die Entstehung fester Materie im Solarnebel und die Entwicklung der Meteoritenmutterkörper. Habilitation thesis. Westfälische Wilhelms-Universität Münster, Münster, Germany.

Bischoff A. 1998. Aqueous alteration of carbonaceous chondrites: Evidence for preaccretionary alteration—A review. *Meteoritics & Planetary Science* 33:1113–1122.

Bischoff A., Palme H., Spettel B., Clayton R. N., and Mayeda T. K. 1988. The chemical composition of dark inclusions from the Allende meteorite. 14th Lunar and Planetary Science Conference. pp. 88–89.

Brearley A. J. 1996. Nature of matrix in unequilibrated chondrites and its possible relationship to chondrules. In C*hondrules and the protoplanetary disk,* edited by Hewings R. H., Jones R. H., and Scott E. R. D. Cambridge: Cambridge University Press. pp. 137–151.

Brearley A. J. and Jones R. H. 1998. Chondritic meteorites. In *Planetary materials,* edited by. Papike J. J. Washington D.C.: Mineralogical Society of America. pp. 3.1–3.398.

Brenker F. E., Palme H., and Klerner S. 2000. Evidence for solar nebula signatures in the matrix of the Allende meteorite. *Earth and Planetary Science Letters* 178:185–194.

Buchanan P. C., Zolensky M. E., and Reid A. M. 1996. Petrology of Allende dark inclusions. *Geochimica et Cosmochimica Acta* 61: 1733–1743.

Bunch T., Schultz P., Cassen P., Brownlee D., Podolak M., Lissauer J., Reynolds R., and Chang S. 1991. Are some chondrule rims formed by impact processes? Observations and experiments. *Icarus* 91:76–92.

Buseck P. R. and Hua X. 1993. Matrices of carbonaceous chondrite meteorites. *Annual Review of Earth and Planetary Science* 21: 255–305.

Busemann H. 1998. Primordial noble gases in "Phase Q" in carbonaceous and ordinary chondrites studied by closed system stepped etching. Ph.D. thesis, Swiss Federal Institute of Technology Zürich, Zürich, Switzerland.

Busemann H., Baur H., and Wieler R. 2000. Primordial noble gases in "phase Q" in carbonaceous and ordinary chondrites studied by closed-system stepped etching. *Meteoritics & Planetary Science* 35:949–973.

Busemann H., Baur H., and Wieler R. 2001. Helium isotopic ratios in carbonaceous chondrites: Significant for the early solar nebula and circumstellar diamonds? (abstract #1598). 32nd Lunar and Planetary Science Conference.

Eberhardt P., Eugster O., and Marti K. 1965. A redetermination of the isotopic composition of atmospheric neon. *Zeitschrift für Naturforschung* 20a:623–624.

Endress M., Keil K., Bischoff A., Spettel B., Clayton R. N., and Mayeda T. K. 1994. Origin of dark clasts in the Acfer 059/El Djouf 001 CR2 chondrite. *Meteoritics* 29:26–40.

Grady M. M. 2000. *Catalogue of meteorites*. Cambridge: Cambridge University Press. 689 p.

Grady M. M., Weisberg M. K., Verchovsky A., Franchi I. A., Pillinger C. T., and Prinz M. 1999. Carbon, nitrogen, and noble gas study of dark inclusions in the Wells ordinary chondrite. *Meteoritics & Planetary Science* 34:A46.

Heymann D. and Mazor E. 1968. Noble gases in unequilibrated ordinary chondrites. *Geochimica et Cosmochimica Acta* 32:1–19.

Housley R. M. and Cirlin E. H. 1983. On the alteration of Allende chondrules and the formation of matrix. In *Chondrules and their origins,* edited by King E. A. Houston: Lunar and Planetary Institute. pp 145–161.

Hua X., Wang J., and Buseck P. R. 2002. Fine-grained rims in the Allan Hills 81002 and Lewis Cliff 90500 CM2 meteorites: Their origin and modification. *Meteoritics & Planetary Science* 37: 229–244.

Huss G. R. and Alexander E. C., Jr. 1987. On the presolar origin of the "normal planetary" noble gas component in meteorites. Proceedings, 7th Lunar and Planetary Science Conference. pp. E710–E716.

Huss G. R. and Lewis R. S. 1994. Noble gases in presolar diamonds I: Three distinct com-ponents and their implications for diamond origins. *Meteoritics* 29:791–810.

Huss G. R. and Lewis R. S. 1995. Presolar diamond, SiC, and graphite in primitive chondrites: Abundances as a function of meteorite class and petrologic type. *Geochimica et Cosmochimica Acta* 59: 115–160.

Huss G. R., Keil K., and Taylor G. J. 1981. The matrices of unequilibrated ordinary chondrites: Implications for the origin and history of chondrites. *Geochimica et Cosmochimica Acta* 45: 33–51.

Huss G. R., Lewis R. S., and Hemkin S. 1996. The "normal planetary" noble gas component in primitive chondrites: Compositions, carrier, and metamorphic history. *Geochimica et Cosmochimica Acta* 60:3311–3340.

Johnson C. A., Prinz M., Weisberg M. K., Clayton R. N., and Mayeda T. K. 1990. Dark inclusions in Allende, Leoville, and Vigarano: Evidence for nebular oxidation of CV3 constituents. *Geochimica et Cosmochimica Acta* 54:819–830.

Kojima T. and Tomeoka K. 1997. Indicators of aqueous alteration and thermal metamorphism on the CV parent body: Microtextures of a dark inclusion from Allende. *Geochimica et Cosmochimica Acta* 60:2651–2666.

Kracher A., Keil K., and Scott E. R. D. 1982. Leoville (CV3)—An accretionary breccia. *Meteoritics* 17:A239.

Kurat G., Palme H., Brandstätter F., and Huth J. 1989. Allende xenolith AF: Undisturbed record of condensation and aggregation of matter in the solar nebula. *Zeitschrift für Naturforschung* 44a:988–1004.

Lewis R. S., Srinivasan B., and Anders E. 1975. Host phase of a strange xenon component in Allende. *Science* 190:1251–1262.

Lewis R. S., Alaerts L., Hertogen J., Janssens M. J., Palme H., and Anders E. 1979. A carbonaceous inclusion from the Krymka LL chondrite: Noble gases and trace elements. *Geochimica et Cosmochimica Acta* 43:897–903.

Leya I., Lange H. J., Neumann S., Wieler R., and Michel R. 2000. The production of cosmogenic nuclides in stony meteoroids by galactic cosmic ray particles. *Meteoritics & Planetary Science* 35:259–286.

MacPherson G. J., Hashimoto A., and Grossman L. 1985. Accretionary rims on inclusions in the Allende meteorite. *Geochimica et Cosmochimica Acta* 49:2267–2279.

Marti K. 1967. Trapped xenon and the classification of chondrites. *Earth and Planetary Science Letters* 2:193–196.

Metzler K. and Bischoff A. 1989. Accretionary dust mantles in CM chondrites as indicators for processes prior to parent body formation (abstract). 20th Lunar and Planetary Science Conference. pp. 689–690.

Metzler K. and Bischoff A. 1996. Constraints on chondrite agglomeration from fine-grained chondrule rims. In *Chondrules and the protoplanetary disk,* edited by Hewings R. H., Jones R. H., and Scott E. R. D. Cambridge: Cambridge University Press. pp. 153–161.

Metzler K., Bischoff A., and Stöffler D. 1992. Accretionary dust mantles in CM chondrites: Evidence for solar nebula processes. *Geochimica et Cosmochimica Acta* 56:2873–2897.

Nakamura T., Nagao K., Metzler K., and Takaoka N. 1999a. Heterogeneous distribution of solar and cosmogenic noble gases in CM chondrites and implications for the formation of CM parent bodies. *Geochimica et Cosmochimica Acta* 63:257–273.

Nakamura T., Nagao K., and Takaoka N. 1999b. Microdistribution of primordial noble gases in CM chondrites determined by in situ laser microprobe analysis: Decipherment of nebular processes. *Geochimica et Cosmochimica Acta* 63:241–255.

Nakasyo E., Maruoka T., Matsumoto T., and Matsuda J. 2000. A laboratory experiment on the influence of aqueous alteration on noble gas composition in the Allende meteorite. *Antarctic Meteorite Research* 13:135–144.

Nier A. O. 1950. A redetermination of the relative abundances of the isotopes of carbon, nitrogen, oxygen, argon, and potassium. *Physical Review* 77:789–793.

Ott U. 2002. Noble gases in meteorites—Trapped components. In *Noble gases in geochemistry and cosmochemistry,* edited by Porcelli D., Ballentine C. J., and Wieler R. Washighton D.C.: Mineralogical Society of America. pp. 71–100.

Ott U., Mack R., and Chang S. 1981. Noble-gas-rich separates from the Allende meteorite. *Geochimica et Cosmochimica Acta* 45: 1751–1788.

Ozima M. and Podosek F. A. 2002. *Noble gas geochemistry.* Cambridge: Cambridge University Press. 286 p.

Sandford S. A., Bernstein M. P., and Swindle T. D. 1998. The trapping of noble gases by the irradiation and warming of interstellar analogs (abstract). *Meteoritics & Planetary Science* 33:A135.

Schultz L. and Franke L. 2000. Helium, neon, and argon in meteorites. A data collection. Update 2000. MPI-Chemie Mainz, Germany.

Scott E. R. D., Rubin A. E., Taylor G. J., and Keil K. 1984. Matrix material in type 3 chondrites—Occurence, heterogeneity, and relationship with chondrules. *Geochimica et Cosmochimica Acta* 48:1741–1757.

Scott E. R. D., Barber D. J., Alexander C. M., Hutchinson R., and Peck J. A. 1988. Primitive material surviving in chondrites: Matrix. In *Meteorites and the early solar system,* edited by. Kerridge J. F. and Matthews M. S. Tucson: University of Arizona Press. pp. 718–745.

Scott E. R. D., Love S. G., and Krot A. N. 1996. Formation of chondrules and chondrites in the protoplanetary nebula. In *Chondrules and the protoplanetary disk,* edited by Hewings R. H., Jones R. H., and Scott E. R. D. Cambridge: Cambridge University Press. pp. 87–96.

Sears D. W. G., Grossman N. J., Melcher C. L., Ross L. M., and Mills A. A. 1980. Measuring metamorphic history of unequilibrated ordinary chondrites. *Nature* 287:791–795.

Sears D. W. G., Batchelor J. D., Lu J., and Keck B. D. 1991. Metamorphism of CO and CO-like chondrites and comparisons with type 3 ordinary chondrites. *Proceedings of the NIPR Symposium on Antarctic Meteorites* 4:319–343.

Sears D. W. G., Benoit P. H., and Jie L. 1993. Two chondrule groups each with distinctive rims in Murchison recognized by cathodoluminiscence. *Meteoritics* 28:669–675.

Semenenko V. P., Bischoff A., Weber I., Perron C., and Girich A. L. 2001. Mineralogy of fine-grained material in the Krymka (LL3.1) chondrite. *Meteoritics & Planetary Science* 36:1067–1086.

Smith P. S., Huneke J. C., Rajan R. S., and Wasserburg G. J. 1977. Neon and argon in the Allende meteorite. *Geochimica et Cosmochimica Acta* 41:627–647.

Tomeoka K. and Kojima T. 1998. Arcuate band texture in a dark inclusion from the Vigarano CV3 chondrite: Possible evidence for early sedimentary processes. *Meteoritics & Planetary Science* 33:519–525.

Tomeoka K. and Tanimura I. 2000. Phyllosilicate-rich chondrule rims in the Vigarano CV3 chondrite: Evidence for parent-body processes. *Geochimica et Cosmochimica Acta* 64:1971–1988.

Vogel N. 2003. Chondrule formation and accretion processes in the early solar nebula—Clues from noble gases in different constituents of unequilibrated chondrites. Ph.D. thesis, Swiss Federal Institute of Technology Zürich, Zürich, Switzerland.

Vogel N., Baur H., Bischoff A., Semenenko V. P., and Wieler R. 2000. Microdistribution of light noble gases in primitive chondrites and implications for their accretionary history (abstract). *Meteoritics & Planetary Science* 35:A165–A166.

Vogel N., Baur H., Bischoff A., Semenenko V. P., and Wieler R. 2001a. Microdistrobution of the noble gases neon and argon in primitive chondrites and implications for their accretionary history (abstract #1841). 32nd Lunar and Planetary Science Conference.

Vogel N., Baur H., Bischoff A., and Wieler R. 2001b. Contrasts in chondrites—Microdistribution of noble gases in Allende, Leoville, and Krymka (abstract). *Meteoritics & Planetary Science* 36:A216.

Vogel N., Baur H., Bischoff A., and Wieler R. 2002. Remnants of solar-like noble gases in chondrules of unequilibrated chondrites? (abstract #1312). 33rd Lunar and Planetary Science Conference.

Weisberg M. K. and Prinz M. 1998. Fayalitic olivine in CV3 chondrite matrix and dark inclusions: A nebular origin. *Meteoritics & Planetary Science* 33:1087–1099.

Wieler R. 2002. Cosmic ray-produced noble gases in meteorites. In *Noble gases in geochemistry and cosmochemistry,* edited by Porcelli D., Ballentine C. J., and Wieler R. Washighton D.C.: Mineralogical Society of America. pp. 125–170.

Wieler R., Graf T., Pedroni A., Signer P., Pellas P., Fieni C., Suter M., Vogt S., Clayton R. N., and Laul J. C. 1989. Exposure history of the regolithic chondrite Fayetteville: II. Solar-gas-free light inclusions. *Geochimica et Cosmochimica Acta* 53:1449–1459.